Louisiana Transportation Research Center

Final Report 488

Repairing/Strengthening of Bridges with Post-tensioned FRP Materials and Performance Evaluation

by

C. S. Cai, Ph.D., P.E.
Miao Xia

Louisiana State University

4101 Gourrier Avenue | Baton Rouge, Louisiana 70808
(225) 767-9131 | (225) 767-9108 fax | www.ltrc.lsu.edu

TECHNICAL REPORT STANDARD PAGE

1. Report No.	2. Government Accession No.	3. Recipient's Catalog No.
FHWA/LA.11/488		

4. Title and Subtitle	5. Report Date
Repairing/Strengthening of Bridges with Post-tensioned FRP Materials and Performance Evaluation	**September 2015**
	6. Performing Organization Code
7. Author(s) C.S. Cai, Ph.D., P.E., Miao Xia	8. Performing Organization Report No.
9. Performing Organization Name and Address Department of Civil and Environmental Engineering Louisiana State University Baton Rouge, LA 70803	10. Work Unit No. 11. Contract or Grant No. LTRC Project Number: 07-3ST SIO: 30000130
12. Sponsoring Agency Name and Address Louisiana Department of Transportation and Development P.O. Box 94245 Baton Rouge, LA 70804-9245	13. Type of Report and Period Covered Final Report Oct. 2007-Aug. 2011 14. Sponsoring Agency Code

15. Supplementary Notes

Conducted in Cooperation with the U.S. Department of Transportation, Federal Highway Administration

16. Abstract

One of the challenges that transportation agencies are facing is to keep bridges in good condition during their service life. Numerous bridges are classified as structurally and/or functionally deficient in the country. In the state of Louisiana, 4,591 bridges, or 34 percent of the total 13,426 bridges, are classified as substandard. Load capacity degradation, increased gross vehicle weight, and increasing traffic demand lead to the deficiencies. One of the most effective ways to solve the problem is to use composite materials to strengthen existing bridges. As rapidly developed over the past several decades, different kinds of composite fiber reinforced polymers (FRP) have been regarded as one of the best solutions to several problems associated with transportation and civil engineering infrastructures. Some of the major benefits of FRP include high strength to weight ratio, high fatigue endurance, excellent corrosion resistance, low thermal expansion, and the ease of fabrication, manufacturing, handling, and installation. The main objective of this research was to develop a flexural resistance designing process using post-tensioning prestressed carbon reinforced polymers (CFRP) laminates adhering to bridge girders to avoid various possible flexural failure modes. It is noted that, in the original plan, a steel bridge and a concrete bridge was to be rehabilitated with prestressed FRP laminates or rods and the bridge performance was to be monitored. However, the sponsor decided not to pursue the field implementation due to cost. This report presents a review of the up-to-date work on bridges strengthened with FRP materials. Mechanical properties of FRP fibers and composites were presented in detail. Investigators presented previous research findings on experiments of FRP composite materials used as various prestressed tendons, and the analyses for different failure modes were introduced. To investigate the effect of rehabilitation with prestressed CFRP laminates, two 3-D finite element analyses were conducted to examine the deflection and bottom fiber stress at the mid-span. A detailed designing process of rehabilitation with prestressed CFRP laminates was presented in this report. A feasible plan to enhance the flexural capability of an existing bridge with externally prestressed CFRP laminates according to AASHTO and ACI code specifications was also proposed in this report.

17. Key Words	18. Distribution Statement
fiber optic sensors, FRP, Prestressing, bridge monitoring, bridge testing, bridge rating, finite element analysis	**Unrestricted. This document is available through the National Technical Information Service, Springfield, VA 21161.**

19. Security Classif. (of this report)	20. Security Classif. (of this page)	21. No. of Pages	22. Price
N/A	N/A	88	N/A

Project Review Committee

Each research project will have an advisory committee appointed by the LTRC Director. The Project Review Committee is responsible for assisting the LTRC Administrator or Manager in the development of acceptable research problem statements, requests for proposals, review of research proposals, oversight of approved research projects, and implementation of findings.

LTRC appreciates the dedication of the following Project Review Committee Members in guiding this research study to fruition.

LTRC Manager

Walid Alaywan, Ph.D., P.E.

Structures Research Manager

Members

Paul Fossier, P.E.

Gill Gautreau, P.E.

Michael Boudreaux, P.E.

Art Aguirre, P.E.

Directorate Implementation Sponsor

Richard Savoie, P.E.

DOTD Chief Engineer

Repairing/Strengthening of Bridges with Post-tensioned FRP Materials and Performance Evaluation

by

C. S. Cai, Ph.D., P.E.
and
Miao Xia

Department of Civil Engineering
Louisiana State University
Baton Rouge, Louisiana 70803

LTRC Project No. 07-3ST
State Project No. 736-99-1438

conducted for

Louisiana Department of Transportation and Development
Louisiana Transportation Research Center

September 2015

ABSTRACT

One of the challenges that transportation agencies are facing is to keep bridges in good condition during their service life. Numerous bridges are classified as structurally and/or functionally deficient in the country. In the state of Louisiana, 4,591 bridges, or 34 percent of the total 13,426 bridges, are classified as substandard. Load capacity degradation, increased gross vehicle weight, and increasing traffic demand lead to the deficiencies.

One of the most effective ways to solve the problem is to use composite materials to strengthen existing bridges. As rapidly developed over the past several decades, different kinds of composite fiber reinforced polymers (FRP) have been regarded as one of the best solutions to several problems associated with transportation and civil engineering infrastructures. Some of the major benefits of FRP include high strength to weight ratio, high fatigue endurance, excellent corrosion resistance, low thermal expansion, and the ease of fabrication, manufacturing, handling, and installation.

The main objective of this research was to develop a flexural resistance designing process using post-tensioning prestressed carbon reinforced polymers (CFRP) laminates adhering to bridge girders to avoid various possible flexural failure modes. It is noted that, in the original plan, a steel bridge and a concrete bridge was to be rehabilitated with prestressed FRP laminates or rods and the bridge performance was to be monitored. However, the sponsor decided not to pursue the field implementation due to cost.

This report presents a review of the up-to-date work on bridges strengthened with FRP materials. Mechanical properties of FRP fibers and composites were presented in detail. Investigators presented previous research findings on experiments of FRP composite materials used as various prestressed tendons, and the analyses for different failure modes were introduced. To investigate the effect of rehabilitation with prestressed CFRP laminates, two 3-D finite element analyses were conducted to examine the deflection and bottom fiber stress at the mid-span. A detailed designing process of rehabilitation with prestressed CFRP laminates was presented in this report. A feasible plan to enhance the flexural capability of an existing bridge with externally prestressed CFRP laminates according to AASHTO and ACI code specifications was also proposed in this report.

ACKNOWLEDGMENTS

The investigators are thankful to the Federal Highway Administration and the Louisiana Transportation Research Center (LTRC) for funding this project. The contents of this report reflect only the views of the writers who are responsible for the facts and the accuracy of the data presented herein. The authors would like to thank those who provided help during the development of the initial tasks of this research program. Special thanks go to the project manager Dr. Walid Alaywan, the Louisiana Department of Transportation and Development (LADOTD), and the entire project review committee.

IMPLEMENTATION STATEMENT

The project is intended to be a direct implementation of research results by using FRP rods as prestressed tendons to strengthen the flexural capacity of existing bridges in Louisiana, thus developing needed expertise and application procedures. The research results may also be presented to state structural and bridge engineers and at the Louisiana American Society of Civil Engineers (ASCE) meeting, Louisiana Transportation Conference, TRB conferences, and in journals. The dissemination of research results will help the future implementation of bridge rehabilitation techniques, and feedback from practical engineers will help judge the progress of implementation.

It is noted that, in the original plan, a steel bridge and a concrete bridge were to be rehabilitated with prestressed FRP laminates or rods and the bridge performance was to be monitored. However, LA DOTD decided not to pursue the field implementation. Later, another bridge was selected and strengthening with carbon fiber composite cables (CFCC) was performed on all six girders on one of the spans while the remaining girders on other spans were strengthened with regular prestressed steel rods. The CFCC cables were instrumented and data will be collected for analysis and performance evaluation under LTRC Research Project No. 13-4ST.

TABLE OF CONTENTS

LIST OF FIGURES

LIST OF TABLES

INTRODUCTION

Background

One of the challenges that transportation agencies are facing is to keep bridges in good condition during their service life. Bridges, as backbones of the highway system, must be maintained and preserved to ensure safety to the traveling public. According to an FHWA report, the average age of bridges has reached over 40, and 167,566 deficient structures within the highway bridge network representing 28.6 percent of the roughly 600,000 bridges in the country are classified as structurally and/or functionally deficient *[1]*. In the state of Louisiana, 4,591 bridges, or 34 percent of the total 13,426 bridges, are classified as substandard. Two reasons lead to the deficiencies. The first one is the load capacity degradation due to the increasing age of the structural components and the aggressive environment bridge structures are exposed to; secondly, the increased gross vehicle weight and vehicular impact damage to the load carrying capacity and safety of existing bridges. In order to rehabilitate or strengthen these bridges, more than $200 billion will be needed to eliminate these structural deficiencies and to restore or improve their load capacity to meet current demand *[2]*.

As rapidly developed over the past several decades, different kinds of composite FRP have been regarded as one of the best solutions to several problems associated with transportation and civil engineering infrastructures. FRP was first used in aerospace, aeronautical, automotive, and other industries, and then was introduced to the civil engineering field decades ago. Some of the major benefits of FRP include high strength to weight ratio, high fatigue endurance, excellent corrosion resistance, low thermal expansion, and the ease of fabrication, manufacturing, handling, and installation.

Among the three categories of FRP materials, namely aramid, carbon, and glass fiber reinforced polymers; CFRP is the most popular one in the civil engineering field. Two types of commercial products of FRP are widely used in civil engineering, laminates, and bars. Obviously, it was more effective to use them as prestressed tendons to reinforce flexural components owing to their high strength and relatively low elastic modulus properties. The aim of the study was to develop a designing process of flexural resistance using post-tensioning prestressed CFRP tendons applied to existing bridges to void various possible flexural failure modes.

Literature Review

Extensive studies and research were conducted in Canada, Europe, Japan, and USA in the last two decades. This section presents a brief summary of state-of-art mechanical properties of FRP materials, flexural behavior, failure mode, and analysis models of structural components strengthened using prestressed FRP materials.

Mechanical Properties

Fibers. Fibers provide the FRP system strength and stiffness, while the resin transfers stress among fibers and protects them. Fibers used for manufacturing composite materials usually have high strength and stiffness, toughness, and durability. The most commonly used fibers for FRPs are carbon, glass, and aramid. Contrary to conventional steel that behaves in an elasto-plastic manner, the FRP product in general behaves in a linear elastic manner and fails at large strains. There is no yielding point before it fails. The mechanical properties are shown in Figure 1 compared with reinforcing steel and resins. Typical mechanical properties of these fibers can also be found in Table 1.

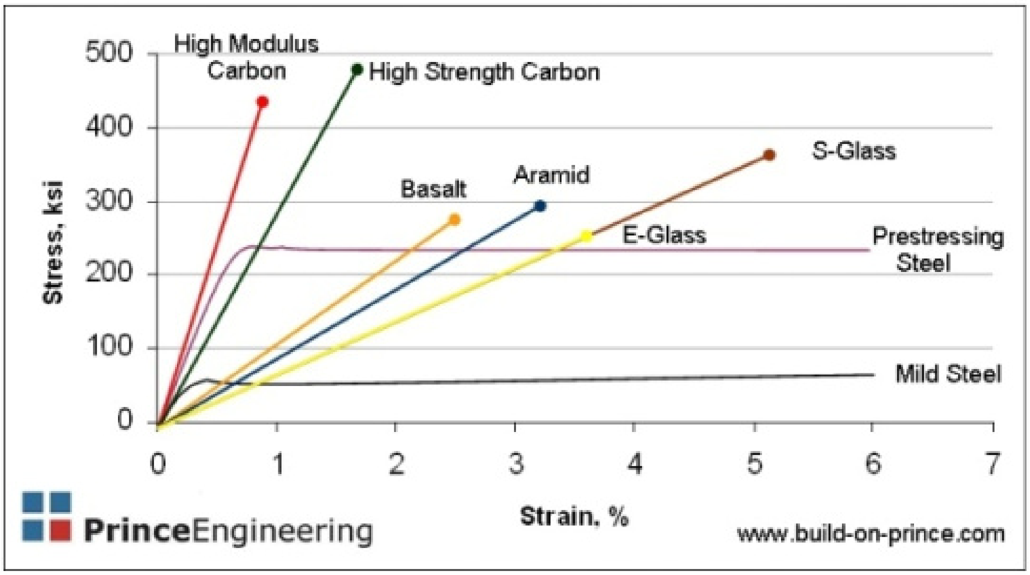

Figure 1
Tensile stress-strain behavior of reinforcing fibers as compared with steel

(adapted from Gerritse and Schurhoff)

Table 1
Typical mechanical properties of fibers

FIBER TYPE		Tensile Strength (MPa)	Modulus Elasticity (GPa)	Elongation (%)	Coefficient of Thermal Expansion (10E-6)	Poisson's Ratio
CARBON						
PAN	High Strength	3500	200-240	1.3-1.8	(-1.2) to (-0.1) (α_frpL), 7 to 12 (α_frpT)	-0.2
	High Modulus	2500-4000	350-650	0.4-0.8		
Pitch	Ordinary	780-1000	38-40	2.1-2.5	(-1.6) to (-0.9) (α_frpL)	N/A
	High Modulus	3000-3500	400-800	0.4-1.5		
ARAMID						
Kevlar 29		3620	82.7	4.4	N/A	0.35
Kevlar 49		2800	130	2.3	2.0 (α_frpL), 59 (α_frpT)	
Kevlar 129		4210 (est.)	110 (est.)	--	N/A	
Kevlar 149		3450	172-179	1.9	N/A	
Twaron		2800	130	2.3	2.0 (α_frpL), 59 (α_frpT)	
Technara		3500	74	4.6	N/A	
GLASS						
E-Glass		3500-3600	74-75	4.8	5	0.2
S-Glass		4900	87	5.6	2.9	0.22
Alkali Resistan Glass		1800-3500	70-76	2.0-3.0	N/A	N/A

(adopted from Design Manual No. 3 Sep. 2001, Reinforcing Concrete Structures with Fiber Reinforced Polymers ISIS CANADA)

Resins System. The resins are other important constituents in composites; they not only coat the fibers and protect them from mechanical abrasion but also transfer stresses between the fibers. The matrixes transfer inter-laminar and in-plane shear in the composite and provide lateral support to fibers against buckling while subjected to compressive loads. Epoxy and polyester are the most commonly used resins. Resins in the manufacture of composites have relatively low strain to failure, resulting in low impact strength. Mechanical properties of some thermo set resins are provided in Table 2.

Table 2
Typical properties of thermosetting resins

Resin	Specific Gravity (MPa)	Tensile Strength (MPa)	Tensile Modulus (GPa)	Cure Shrinkage (%)
Epoxy	1.20-1.30	55.00-130.00	2.75-4.10	1.00-5.00
Polyester	1.10-1.40	34.50-103.50	2.10-3.45	5.00-12.00
Vinyl Ester	1.12-1.32	73.00-81.00	3.00-3.35	5.40-10.30

(adopted from Design Manual No. 3 Sep. 2001, Reinforcing Concrete Structures with Fiber Reinforced Polymers ISIS CANADA)

To resist the aggressive service condition, the FRP system selected should include a resin matrix resistant to alkaline, acidic or other special environments *[3]*.

FRP Reinforcing Products and Material Properties. FRP materials are composed of a number of continuous fibers, bundled in a resin matrix. FRP tendons are available in the form of rods or cables, rectangular strips, braided rods, and multi-wire strands. Normally, the volume fraction of fibers in FRP strips is about 50-70 percent and that in FRP fabrics is about 25-35 percent. The mechanical properties of the final FRP product depend on the types and quality of fibers, fiber to resin volumetric ratio, orientation, shape, fiber adhesion to the matrix, and the manufacturing process. The tensile behaviors of FRP bars are similar to FRP fibers, when loaded in tension. They are characterized by a linearly elastic stress-strain relationship until failure without exhibiting any plastic behavior. The kind of fiber and the fiber to overall volumetric ratio affect the mechanical properties of FRP materials most because fibers are the main load-carrying constituents, while the resin transfers stresses among fibers and protects them. The tensile properties of some commonly used FRP bars are shown in Table 3 compared with steels. Figure 2 demonstrates the tensile strain stress behaviors of construction materials (FRP, steel, and concrete). Compared with Figure 1, the Young's modulus of FRP composite materials is always smaller than that of steels; even though the Young's modulus of fibers is usually larger than that of steels.

Table 3
Tensile properties of FRP bars (ACI 440.2R-02)

	Steel	GFRP	CFRP	AFRP
Nominal yield stress, ksi (Mpa)	40-75 (276-517)	N/A	N/A	N/A
Tensile strength, ksi (Mpa)	70-100 (483-690)	70-230 (483-1600)	87-535 (600-3690)	250-368 (1720-2540)
Elastic modulus, x10E3 ksi (Gpa)	29 (200.0)	5.1-7.4 (35.0 to 51.0)	15.9-84.0 (120.0-580)	6.0-18.2 (41.0-125.0)
Yield strain, %	1.4-2.5	N/A	N/A	N/A
Rupture strain, %	6.0-12.0	1.2-3.1	0.5-1.7	1.9-4.4

Note: Typical values for fiber volume fractions ranging from 0.5 to 0.7

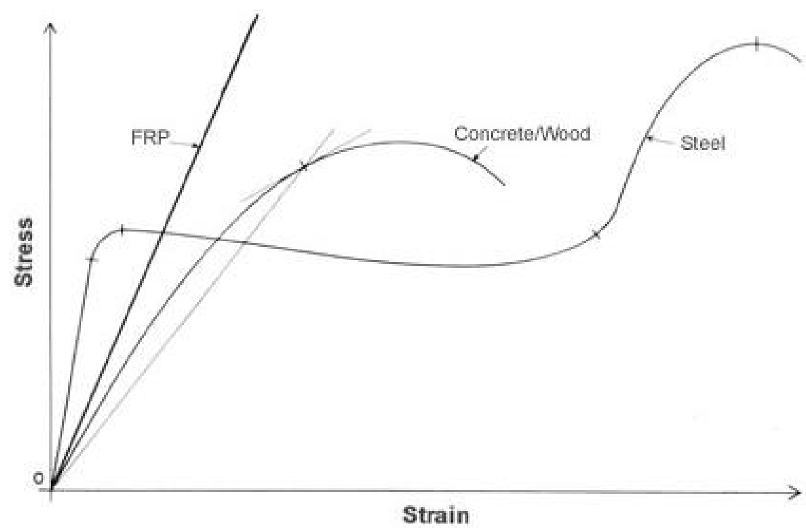

Figure 2
Tensile stress-strain behaviors of construction materials

(adopted from Ambrose)

When FRP materials are subjected to a constant stress, they can fail suddenly. This phenomenon is referred to as creep rupture that exists for all structural materials including steel. In general, carbon fibers are the least susceptible to creep rupture; aramid fibers are moderately susceptible, and glass fibers are most susceptible. The creep rupture happens due to resins not fibers; therefore, the orientation and volume of fibers have a significant influence on the creep performance of tendons. Studies on glass FRP (GFRP) composites indicate that stress rupture diminishes if the sustained loads are limited to 60 percent of the short-term strength while that of prestressing steel is 75 percent. Figure 3 shows the variation of strength of FRP subjected to a long term load *[4]*.

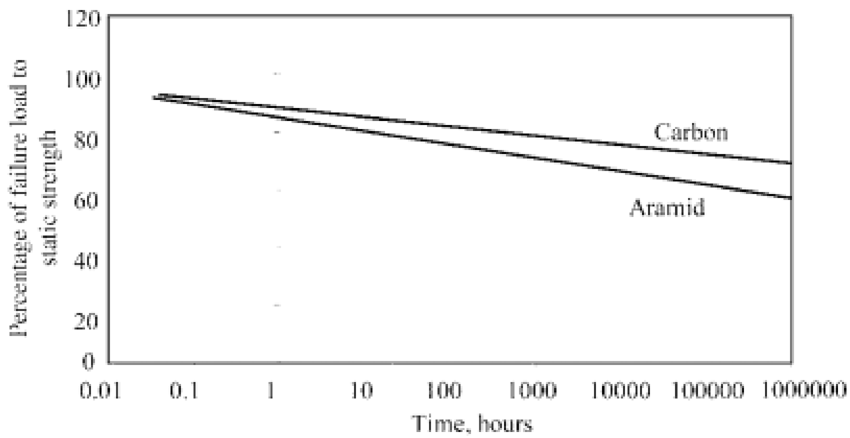

Figure 3
Comparison of creep-rupture curve for aramid and carbon FRP rods under environmental exposure

(adopted from Prestressing Concrete Structures with FRP Tendons, reported by ACI Committee 440)

CFRP and GFRP bars exhibit good fatigue resistance. Research on FRP composites made of high-performance fibers for aerospace applications shows that carbon-epoxy composites have better fatigue strength than steel; while the fatigue strength of glass composites is lower than steel.

Concrete Flexural Components Prestressed with FRP Materials

The structural systems strengthened with externally bonded FRP laminates combine the benefits of mechanical properties of FRP composites, the compressive characteristics of concrete, and the ductility and deformation capacity of steel. This improves the load capacity of the structure. The main advantages are shown in a technical report by the Fédération de l'Industrie du Béton (FIB Bulletin 14) as follows *[5]*:

a. Control the deflection at the early stage and provide stiffer behavior.

b. Delay crack formation in the shear span.

c. Close pre-existing cracks.

d. Improve serviceability and durability due to reduced cracking.

e. Improve the shear resistance of members.

f. Achieve the same strengthening with smaller areas of FRP reinforcement.

g. Achieve greater structural efficiency as the neutral axis remains at a lower level in the prestressed case.

h. Yielding of the internal steel begins at a higher applied force compared to non-prestressed member.

Besides these, there are two other advantages of FRP materials being used as prestressed reinforcement. One is the unloading of the steel reinforcement, which is beneficial for fatigue resistance of the structure because stress in the steel can be maintained at a relatively low stress level. The other one is that, due to the excellent corrosion resistance of FRP, it can be easily used as externally prestressed reinforcements with minor protection.

Numerous studies have been carried out on flexural components strengthened with FRP materials. Experimental studies revealed the behavior of beams strengthened with FRP composites by means of different methods *[6-15]*. Failure modes were identified based on these experiments *[16-18]*. Calculation formulas were established and load capacity estimation was developed based on the mechanical models simplified from failure modes *[6, 19-21]*. A special failure mode, the debonding of FRP composite off the surface of concrete, was investigated in detail *[22-24]*. Long-term and time-dependent performance were also evaluated *[25-27]*.

Badawi and Soudki investigated the effectiveness of strengthening reinforced concrete (RC) beams with prestressed near-surface mounted (NSM) CFRP rods *[9]*. In their study, four RC beams that are 10 in. (254 mm) deep by 6 in. (152 mm) wide by 11.5 ft. (3500 mm) long were tested under monotonic loading including an un-strengthened control beam and a beam with non-prestressed NSM CFRP rods. The setup of the experiment is shown in Figure 4. Strain gages were placed on the concrete, the FRP rod, and reinforcing bars. Strain profile versus beam depth using strain readings show that, similar to ordinary RC beams, beams strengthened with prestressed NSM CFRP rods satisfy the plane-section assumption, i.e., a cross section that was plane before loading remains plane under load as shown in Figure 5.

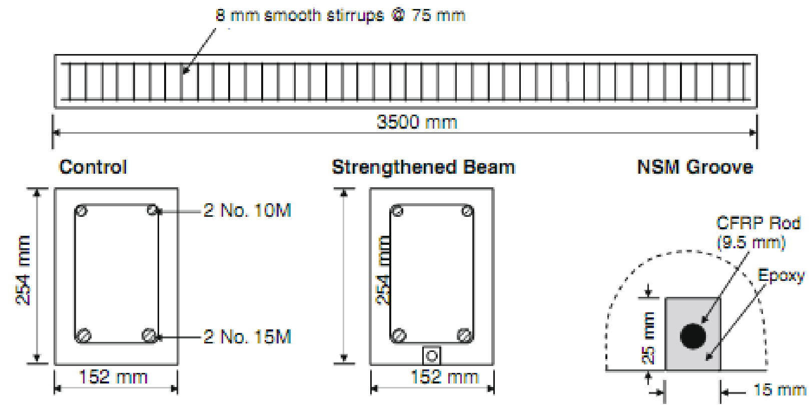

Figure 4
Specimen design

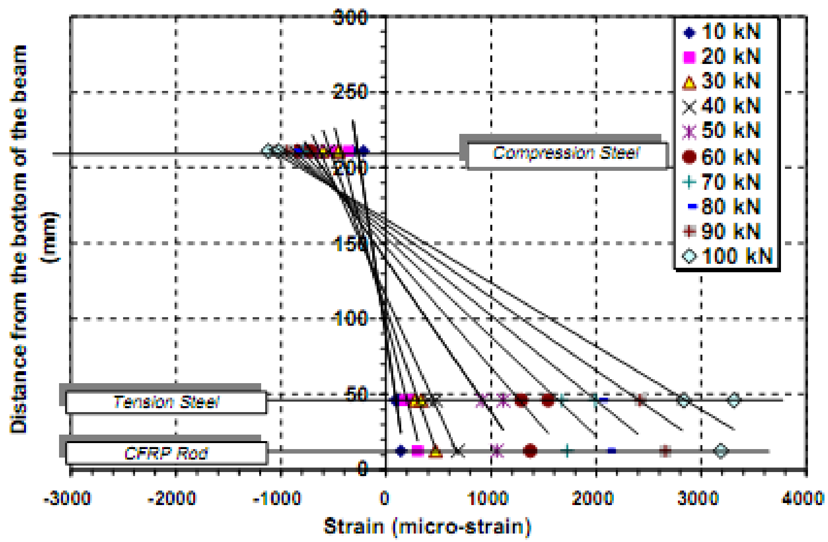

Figure 5
Typical strain profiles during loading (60 percent prestressed)

The first one is characterized with concrete crushing at the top fiber of the cross-section after yielding of the tension steel reinforcement. With respect to capacity, it showed that compared with the control beam, the RC beams strengthened with prestressed (40 percent and 60 percent) NSM CFRP rods increased their yield and ultimate capacity by 90 percent and 79 percent, respectively. The failure mode of prestressed CFRP rods is characterized with rupture in the CFRP rod after yielding of the tension steel reinforcement.

Mukherjee and Rai conducted a study on the flexural behavior of RC beams that have reached their ultimate bearing capacities and then retrofitted with externally prestressed carbon fiber reinforced composite (CFRC) laminates *[7]*. The RC beams were first damaged with a four point bending test. It was observed that the failure mode of the beams was due to yielding of the tension steel prior to the application of any CFRC. And then, the CFRP laminates were pulled to the desired tensile force and bonded to the tension face of the beam with a specially designed machine thereafter. To avoid peeling off of CFRC laminates, the ends of laminates were secured by means of a wrap of the CFRC sheet. Therefore, due to the rehabilitation of the bending capacity, the failure mode shifts to crushing of concrete in the compression zone and the beams were fully utilized. The load-mid-span deflection curves of the beam at all the different phases of the test are shown in Figure 6. It is noted that the failure did not lead to a sudden loss of stiffness as commonly expected due to the compression failure of the concrete.

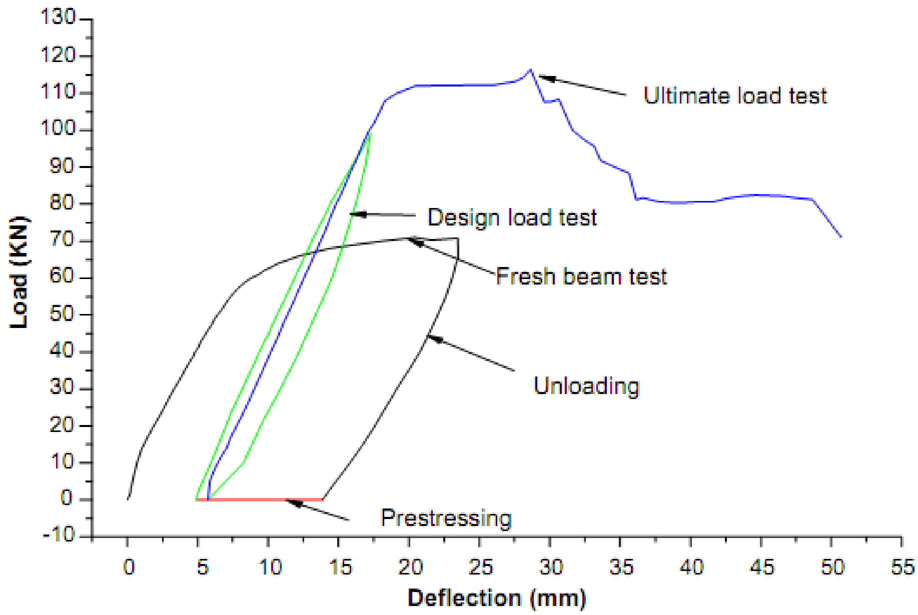

Figure 6
Deflection versus load

Stoll et al. carried out research that involved the design, fabrication, and testing to failure of bridge beams strengthened with FRP products for prestressing and shear reinforcement *[14]*. They noted that, for different manufacturer-supplied CFRP products, the ratios of guaranteed-strength to ultimate-strength are different. Thus, there is not a consistent methodology in use by different tendon manufacturers to establish a characteristic strength value. Two 40-ft. (12.19 m) long AASHTO Type 2 beams were built using different high-strength concrete formulations, and the 28-day compressive strength of cylinders were 12.5 ksi (86.3 MPa) and 10.3 ksi (71.1 MPa), respectively. The Leadline cables were used as prestressing cables. The standard cross-section of an AASHTO Type 2 beam is shown in Figure 7. These two beams were tested to ultimate failure in four-point bending. Both beams failed due to tension failure of the CFRP tendons in the bending zone between the load points and exhibited extensive cracking and large deflections before the failure of the tendons, as shown in Figure 8.

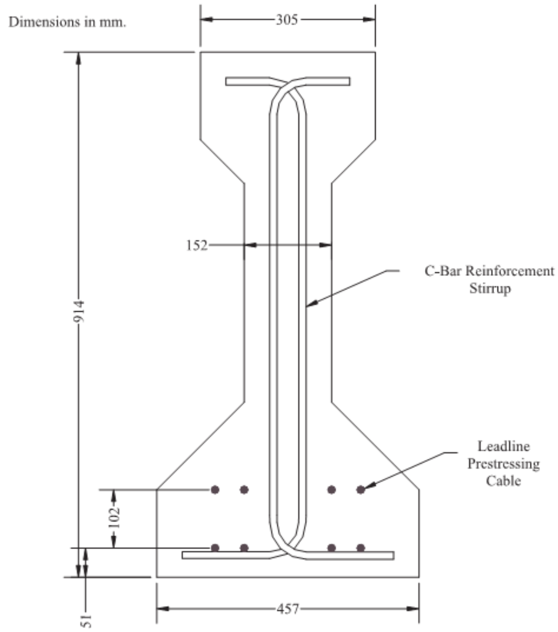

Figure 7
AASHTO Type 2 beam cross-section with prestress and stirrup designs

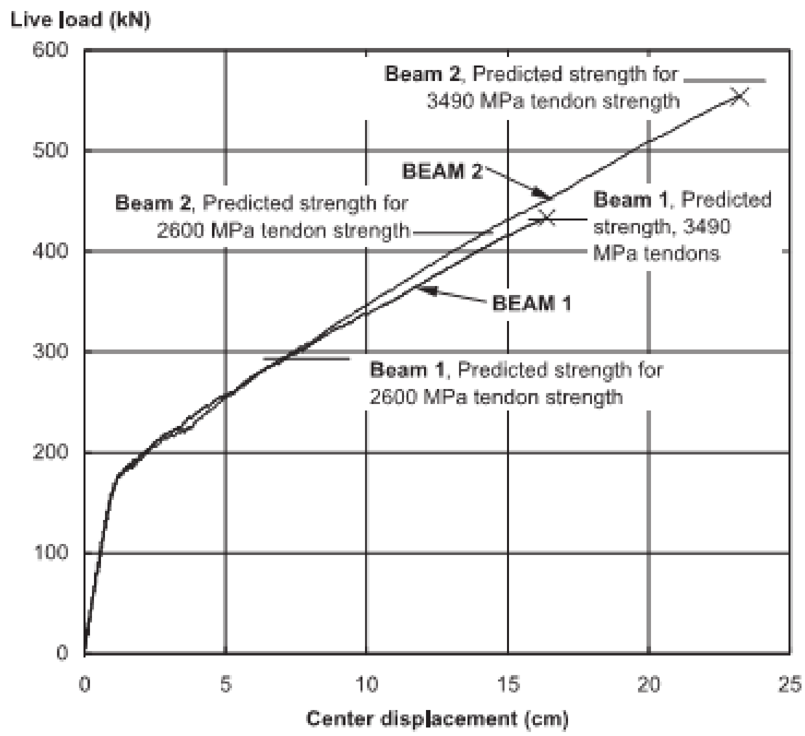

Figure 8
Live load and center displacement test results for the beams compared with predicted strength values

Externally prestressed tendons can improve load carrying capacity of composite beams too. Chen and Gu carried out a study on the ultimate moment and incremental tendon stress of steel-concrete composite beams prestressed with external tendons under positive moment *[28]*. Two beams, prestressed and non-prestressed, were tested for comparison. The non-prestressed beam was loaded to the yielding of the bottom flange and was unloaded. The beam was prestressed thereafter, and then loaded to ultimate failure. The ultimate stress increment in tendons was a substantial factor in the design of composite beams prestressed with external tendons. In their research, the ultimate stress increment in the tendons was expressed in terms of ratio of prestress–span to deflection and is shown in Figure 9. The experimental investigation showed that adding prestressed tendons to composite beams significantly increased both the yield and ultimate flexural capacity and led to less deflection.

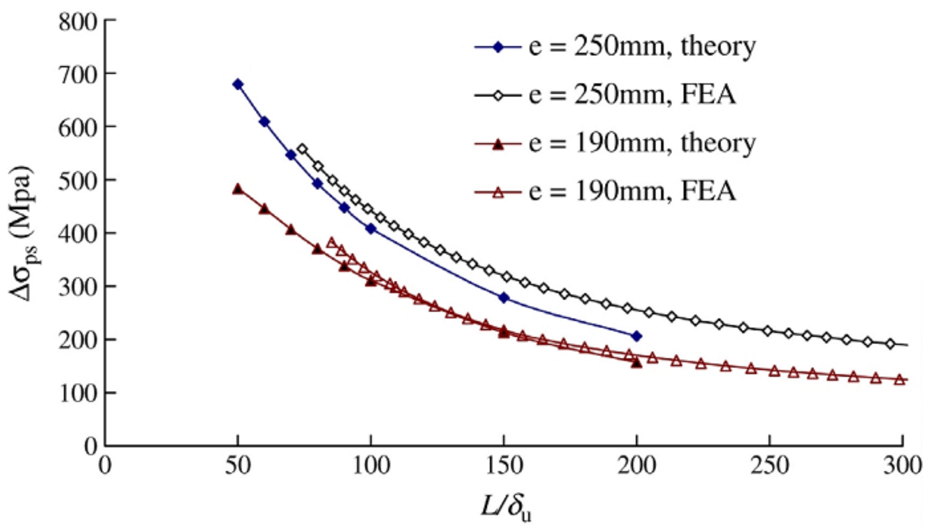

Figure 9
Incremental prestress–span/deflection curves with different eccentricities

Park et al. investigated the improvement of flexural capacity and the effect of a deviator when a steel I-beam member was strengthened with externally unbounded prestressing tendons *[29]*. Four point loading tests were conducted for steel I-beam members strengthened with external steel bars and strands. The setup of the experiments is shown in Figures 10 and 11. As expected, the flexural capacity was improved significantly when the external post-tensioning technique was applied, when the draped tendon was utilized.

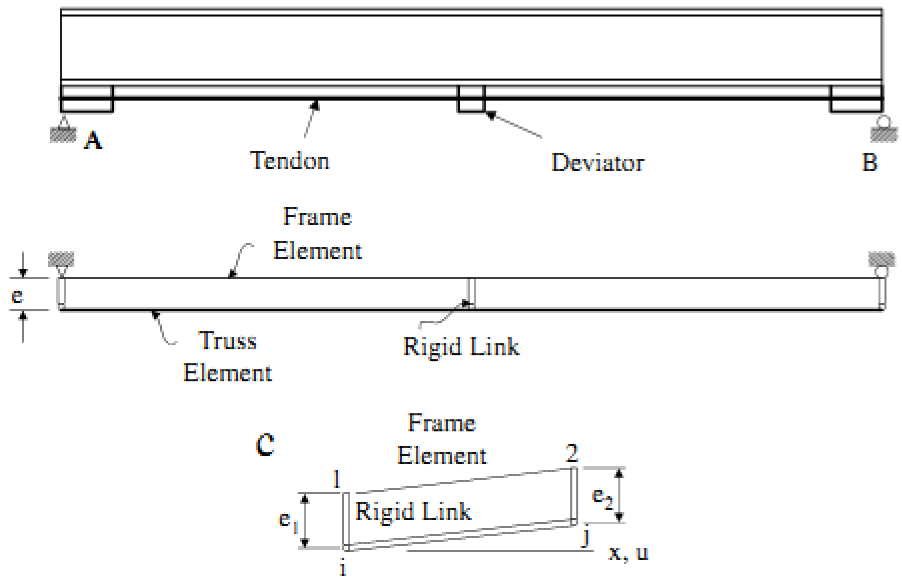

Figure 10
Steel I-beam prestressed with straight tendons

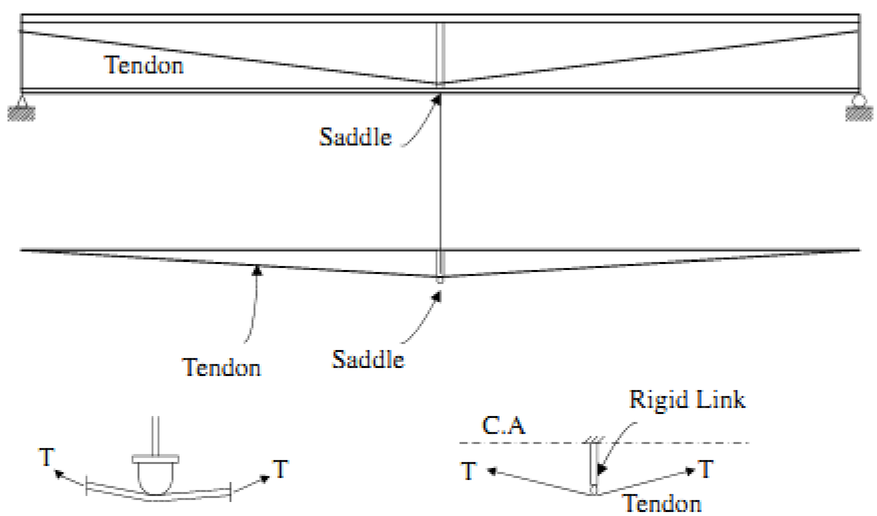

Figure 11
Steel I-beam prestressed with draped tendons

OBJECTIVE

The corrosion of steel reinforcement, both prestressing tendons and non-prestressed rebars, caused by the infiltration of waterborne de-icing agents, is one of the primary sources of a structure's deterioration. The primary solution today in the US is protecting the steel reinforcement with epoxy coatings and protecting the prestressing strands with grouting. Recently, high performance concrete is also being used in the US frequently to help with concrete structure durability. Replacing the metallic reinforcement and strands with FRP composite materials may be a more positive solution. If it significantly increases the bridge life, the increased cost of the nonmetallic reinforcement, strands bars, cables, or grids may be justified. Several experimental and demonstration projects using FRP strands are in service in the US.

The proposed project took advantage of some new developments in bridge engineering to initiate a demonstration bridge with FRP post-tensioning laminates/strands/rods in the state of Louisiana. Specifically, researchers proposed to use externally post-tensioned FRP laminates/strands/rods to repair/strengthen bridges and use a fiber optic sensor (FOS) system to monitor and evaluate the long-term performance of the bridge system. The ultimate objective was to take advantage of the promising FRP materials to develop a more durable, less maintenance intensive bridge system to save the limited budget for other urgent needs of the transportation infrastructure system. It is noted that, in the original plan, a steel bridge and a concrete bridge were to be rehabilitated with prestressed FRP laminates or rods and the bridge performance was to be monitored. However, the sponsor decided not to pursue the field implementation due to cost and this report summarizes the current work by the research team. The present study only served as a preliminary investigation for the ultimate objective.

SCOPE

To achieve the research objective, the scope of work included designing and/or checking the bridge repairing/strengthening scheme with FRP strands, finite element prediction, performance evaluation through laboratory and bridge field testing (original plan), and development of long-term monitoring strategies. This scope of work was changed during the research process under the mutual agreement between the research team and the LADOTD project management team. A bridge for FRP repairing/strengthening applications was selected and provided by LADOTD to the research team.

Literature Review

The researchers examined and reviewed the current technology and state-of-the-art practice regarding the application of FRP strands in bridges, especially post-tensioned FRP strands. This information was gathered from journals, research reports, and other avenues. More specifically, researchers searched topics on common design requirements, code specification and/or design guidelines, research findings from analytical studies, and physical testing.

Tentative Rehabilitation Designing Process with Prestressed CFRP Materials

A tentative designing process included the selection of the type of CFRP materials (bars, tendons, or strips), determination of the amount of the CFRP material and the initial prestress in it, and evaluation of the feasibility of the construction.

3-D Finite Element Analysis of Bridge with FRP Strands

Two 3-D finite element models have been developed to simulate the performance of the selected bridge. The post-tensioned FRP strands have then been designed with an HL-93 load. The dynamic impact effect was represented with an equivalent static load per AASHTO specifications.

METHODOLOGY

The mechanical analysis using fundamental assumptions relating to flexure used in calculating the nominal flexural for reinforced concrete girders and 3-D finite element analysis were conducted for the selected bridge.

Description of the Selected Bridge

The superstructure of the LA 415/Missouri Pacific Railroad overpass on US 190 is located in West Baton Rouge Parish and was constructed in 1940. It is a grade-crossing structure of the federal highway system and a National Bridge Inventory (NBI) structure. The structure consists of 20 cast-in-place concrete T beam approach spans, each is 38 ft. (11.58 m) long, and five steel I-beam spans in the main crossing section, namely one 64-ft., 6-in. (19.66-m), two 38-ft. (11.58-m), and two 47-ft. (14.33-m) spans. All the beams are simply supported between the piers. Other information is given below:

1. Bridge Total Length: 994 ft. and 6 in. (303.12 m)
2. Number of Spans: 25
3. Roadway Width: 2@23 ft. and 9 in. (2@ 7.24 m)
4. Number of Traffic lanes: 2
5. Shoulder Widths: None
6. Sidewalks: 1 ft. and 2 in. (0.36 m)
7. Design Load: H15

According to the latest LADOTD Bridge Inspection Report (dated 05/01/2007), no significant section loss that warrants a reduction in the capability of the primary load carrying members was indicated. Also included in the inspection report was documentation of cracks and spalls in the concrete decks resulting in exposure of the reinforcing steel throughout the structure. Additionally the inspection report indicated the presence of corrosion in some areas of the steel bridge members. Since this structure was built before 1950, the weight of the concrete rail was assumed to be distributed equally to each beam. Figures 12 and 13 show the overview of the bridge.

Figure 12
Steel span and concrete span

Figure 13
Steel span

The analyses were based upon material properties as shown on the Manual for *Condition Evaluation of Bridges* and are noted below *[33]*:

Super Deck:	Class A Concrete Compressive Strength	$f'_c = 3000$ psi
	Deformed Reinforcing Steel Yield Strength	$F_y = 33000$ psi
Steel Beams:	Silicon Steel Yield Strength	$F_y = 41000$ psi

Standards: AASHTO LRFD Bridge Design Specifications (4th Edition, 2007 Interims)

Flexural Capability Examination

Complete analysis of girders of two typical spans, a 38-ft. (11.58-m) concrete deck approach span and a 64.5-ft. (19.66-m) steel I-beam span in the main crossing section, are presented in this report. All the calculations in this analysis use U.S. customary units.

Cast-in-place Concrete Tee Beam Approach Span

The bridge has 20 concrete deck approach spans of equal length, 38 ft., (11.58 m) and each span consists of 10 girders with spacing of 6 ft. (1.83 m) between the exterior and interior girders and 5 ft. (1.52 m) between the interior girders.

Cross-section Determination. The girders are classified as interior (In), exterior (E), and interior-exterior (I-E) and are stiffened by end and intermediate diaphragms at the middle point. The cross-section of the concrete deck approach span is shown in Figure 14.

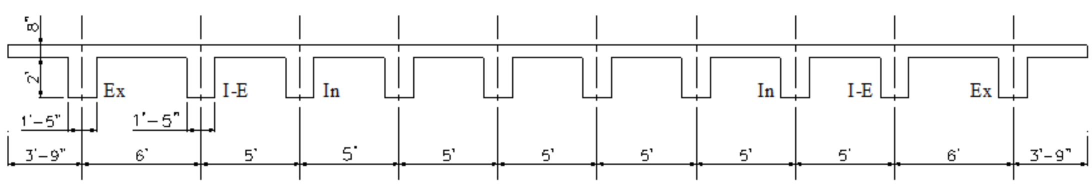

Figure 14
Layout of girders of concrete deck approach span

Two possible critical girders, exterior girders, and interior-exterior girders were examined with respect to the flexural limit states in this report. The cross-sections of these two girders are shown in Figure 15 and their cross-section properties are listed in Table 4.

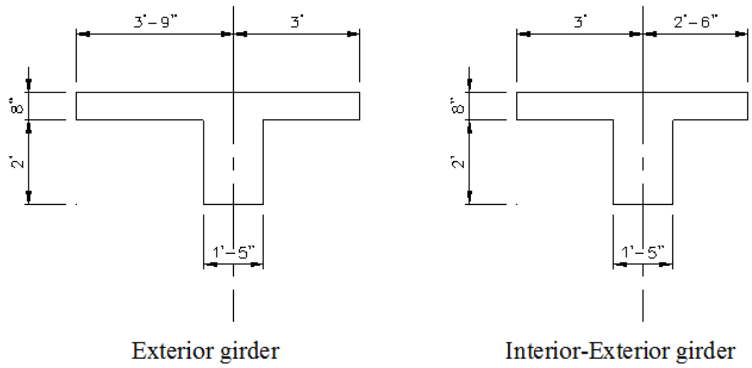

Figure 15
Cross-section of exterior and interior-exterior girders on cast-in-place concrete tee beam approach span

Table 4
Cast-in-place concrete tee beam span cross-section properties

Parameter	Exterior girder	In-exterior girder
Height of section, d (in)	32	32
Deck thickness (in)	8	8
Effective flange width, be (in)	81	66
Area, A (in^2)	1056	936
Moment of inertia (in^4)	85,986	80,329
Natural axis height, y (in)	21.818	21.026
Bottom section modulus, S_b (in^3)	3,941	3,821
Top section modulus, S_t (in^3)	8,445	7,320

Live Load Distribution Factor for Moment. Table 4.6.2.2b-1 in AASHTO LRFD Bridge Design Specification (2007) lists the common deck superstructure type for which approximate live load distributions equations have been assembled. The cross section for this span is type (e). To ensure that approximate distribution equations can be used, several parameters need to be checked:

1. 3.5 ft. < beam spacing < 16 ft. (1.07 m < beam spacing < 4.88 m)
2. 4.5 in. < slab thickness < 12 in. (0.11 m < slab thickness < 0.30 m)
3. 20 ft. < span length < 240 ft. (6.10 m < slab thickness < 73.15 m)
4. 4 < number of girders

The distribution factor for moment in interior beams was taken as follows, for one design lane loaded:

$$gM = 0.06 + \left(\frac{S}{14}\right)^{0.4}\left(\frac{S}{L}\right)^{0.3}\left(\frac{K_g}{12.0Lt_s^3}\right)^{0.1} \tag{1}$$

for two or more design lanes loaded:

$$gM = 0.075 + \left(\frac{S}{9.5}\right)^{0.6}\left(\frac{S}{L}\right)^{0.2}\left(\frac{K_g}{12.0Lt_s^3}\right)^{0.1} \tag{2}$$

in which:

$$K_g = n\left(I + Ae_g{}^2\right) \tag{3}$$

where:

$$n = \frac{E_B}{E_D} \tag{4}$$

E_B = modulus of elasticity of beam material (ksi),
E_D = modulus of elasticity of deck material (ksi),
I = moment of inertia of beam (in^4),
eg = distance between the centers of gravity of the basic beam and deck,
S = spacing of beams (ft.),
A = cross-section area of beam (in^2), and
t_s= depth of concrete slab (in.).

The distribution factor for moment in exterior beams can be derived though lever rule for one lane and by multiplying a factor "e" by the interior girder distribution factor for two or more lanes. Value "e" is defined as following equation:

$$e = 0.77 + \frac{d_e}{9.1} \tag{5}$$

A summary of distribution factor for moment is listed in Table 5.

Table 5
Summary of distribution factor for moment for cast-in-place concrete T-beam

Location	One Lane	Multiple Lanes	Control
Interior-exterior girders	0.458	0.580	0.580
exterior girders	0.6	0.626	0.626

Load Effect on Girders. Two load combinations were considered: strength I and service I. The following load modifiers were used for this calculation:

$\eta_D = 1 \quad \eta_R = 1 \quad \eta_I = 1$

The HL-93 truck was used as a design load. Dynamic load allowance *IM* = 33 percent is used. The bending moments were obtained with a line girder model of a bridge. They are summarized in Table 6.

Table 6
Bending moment summary of cast-in-place concrete tee beam (kip-ft/beam)

Section x/L	Distance	M_{cb} (kip ft)		M_{fw} (kip ft)		M_{bar} (kip ft)	M_{truck} (kip ft)	M_{lane} (kip ft)
		int-ext.	ext.	int-ext.	ext.			
0	0	0	0	0	0	0		0
0.1	3.8	63.36	71.48	8.93	10.97	5.69		41.59
0.2	7.6	112.63	127.07	15.88	19.49	10.12		73.93
0.3	11.4	147.83	166.78	20.85	25.59	13.28		97.04
0.4	15.2	168.95	190.61	23.83	29.24	15.18		110.9
0.5	19	175.99	198.55	24.82	30.46	15.81	394.67	115.52
0.56	21.33	173.33	195.56	24.44	30	15.57	414.32	113.78
0.6	22.8	168.95	190.60	23.83	29.24	15.18		110.9
0.7	26.6	147.83	166.78	20.85	25.59	13.28		97.04
0.8	30.4	112.63	127.07	15.88	19.49	10.12		73.93
0.9	34.2	63.36	71.48	8.93	10.97	5.69		41.59
1	38	0	0	0	0	0		0

Where, M_{cb}, M_{fw}, M_{bar}, M_{truck}, and M_{lane} are moments due to beam self-weight, future wearing surface, barrier self-weight, truck load, and lane load.

Strength I combination $(\mathbf{1.25} \times \boldsymbol{DL} + \mathbf{1.75} \times \boldsymbol{LL})$

For exterior girders (impact factors included), $M_{T\_e} = 1048.734\ kip\ ft$

For interior-exterior girders, $M_{T\_i} = 962{,}114\ kip - ft$

Service I combination $(\mathbf{1.00} \times \boldsymbol{DL} + \mathbf{1.00} \times \boldsymbol{LL})$

$M_{S\_e} = 580.78\ kip\ ft\ and\ M_{S\_i} = 531.224\ kip - ft$

Flexural Capability. Reinforcement arrangement is shown in Figure 16. The nominal moment of exterior girders is determined as follows.

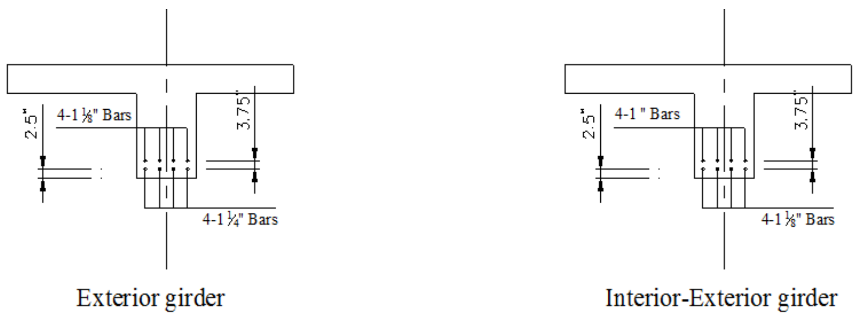

Figure 16
Reinforcement arrangement in girders

As = 9.8 in^2

Distance from the top of the deck to the center of the reinforcement

$$d_e = 32 - \frac{4 \times 1.27 \times 2.5 + 4 \times 1.00 \times (2.5 + 3.75)}{A_s} = 27.85\ in.$$

$$d_i = 32 - \frac{4 \times 1.00 \times 2.5 + 4 \times 1.00 \times (2.5 + 3.75)}{A_s} = 27.63\ in.$$

the depth of compressing concrete

$$a_e = \frac{A_s \times f_y}{0.85 f_c' \times b_e} = 1.76\ in.$$

the nominal moment of exterior girders

$$M_{ne} = A_s f_y \left(d_e - \frac{a_e}{2}\right) = 837.12\ kip - ft.$$

Similarly, the nominal moment of interior-exterior girders can be obtained.

$$M_{ni} = A_s f_y \left(d_i - \frac{a_i}{2}\right) = 774.65\ kip - ft.$$

Since the design load was changed from H15 to HL-93, both the exterior and the interior-exterior girders' flexural capability are insufficient compared to the current traffic requirements.

Steel I-beam Span

The structure incorporates one 64-ft., 6-in. (19.66-m), two 38-ft. (11.58-m), and two 47-ft. (14.33-m) steel I-beam spans in the main crossing section. In this examination, the flexural capability of the longest span, the 64-ft., 6-in. (19.66-m) span is calculated. The span consists of 10 girders with spacing of 7 ft. (2.13 m) between the exterior and interior girders and 5 ft. (1.52 m) between the interior girders simply supported between the steel floor beams.

Steel I-beam Cross-section Determination. The girders are classified as interior (In), exterior (E), and interior-exterior (I-E) and are stiffened by end and intermediate diaphragms. The cross-section of the steel span is shown in Figure 17.

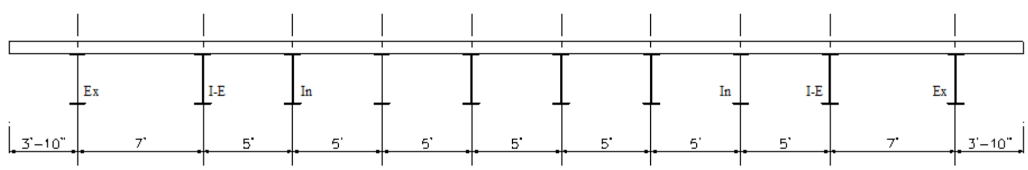

Figure 17
Layout of steel I-beam span

Same as the concrete deck approach span, two possible critical girders, exterior girders and interior-exterior girders were examined with respect to the flexural limit states in this report. The cross-sections of these two girders are shown in Figure 18 and their cross-section properties are listed in Table. 7.

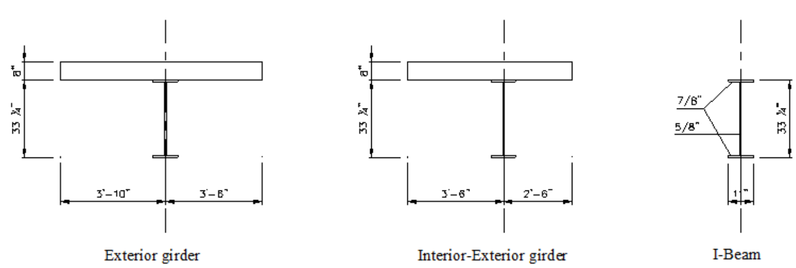

Figure 18
Cross-section of exterior and interior-exterior girders on I-beam steel span

Table 7
Steel I-beam span cross-section properties

Parameter	Exterior girder		In-exterior girder		I-Beam
	Short-term properties	Long-term properties	Short-term properties	Long-term properties	
Height of section, d (in)	41.25	41.25	41.25	41.25	33.25
Deck thickness (in)	8	8	8	8	
Effective flange width, be (in)	88	88	72	72	
Area, A, (in^2)	122.94	66.94	98.94	58.94	38.94
Moment of inertia (in^4)	18,439	13,751	17,038	12,401	6,673
Centroidal axis height, y (in)	30.72	25.25	29.13	23.62	16.625
Bottom section modulus, Sb (in^3)	600.27	544.55	584.84	524.92	401.4
Top section modulus, St (in^3)	1,751	859.59	1,406	703.54	401.4

Live Load Distribution Factor for Moment. According to Table 4.6.2.2.1-1 in the AASHTO LRFD Bridge Design Specifications, the cross section for this span is type (a). The live load distribution factor can be derived from equations (1) - (5). A summary of the distribution factor for the moment for steel I-beam girders is listed in Table 8.

Table 8
Summary of distribution factor for moment for Steel I-beam girders

Location	Parameter	One lane	Multiple lane	Control
Interior-exterior	Moment	0.385	0.513	0.513
	Fatigue moment	0.321		0.321
exterior	Moment	0.600	0.534	0.600
	Fatigue moment	0.500		0.500

Load Effect on Girders. Two load combinations were considered: strength I and service I. The following load modifiers were used for this calculation:

$\eta_D = 1 \quad \eta_R = 1 \quad \eta_I = 1$

The HL-93 truck was used as the design load. A dynamic load allowance of *IM = 33* percent was used. The bending moments were obtained with a line girder model of a bridge. They are summarized in Table. 9.

Table 9
Bending moment summary of steel I-beam girders (kip-ft/beam)

Section x/L	Distance (ft)	M_{beam}	M_{deck}		M_{fw}		M_{bar}	M_{truck}	M_{lane}
			in-ext	Ext	in-ext	ext			
0	0	0	0	0	0	0	0		0
0.1	6.4	24.42	112.07	133.57	28.02	33.39	16.15		117.96
0.2	12.8	43.42	199.23	237.46	49.81	59.37	28.7		209.72
0.3	19.2	56.98	261.49	311.66	65.37	77.92	37.68		275.25
0.4	25.6	65.12	298.84	356.19	74.71	89.05	43.06		314.57
0.5	32	67.84	311.30	371.03	77.82	92.76	44.85	826.7	327.68
0.536	34.333	67.48	309.64	369.06	77.41	92.26	44.61	862.7	325.94
0.6	38.4	65.12	298.84	356.19	74.71	89.05	43.06		314.57
0.7	44.8	56.98	261.49	311.66	65.37	77.92	37.68		275.25
0.8	51.2	43.42	199.23	237.46	49.81	59.37	28.7		209.72
0.9	57.6	24.42	112.07	133.57	28.02	33.39	16.15		117.96
1	64.5	0	0	0	0	0	0		0

Strength I combination $(\mathbf{1.25} \times \boldsymbol{DL} + \mathbf{1.75} \times \boldsymbol{LL})$

For exterior girders (impact factors included), $M_{T\_e} = 2307.014\ kip - ft$

For interior-exterior girders, $M_{T\_i} = 1987.038\ kip\ ft$

Service I combination $(\mathbf{1.00} \times \boldsymbol{DL} + \mathbf{1.00} \times \boldsymbol{LL})$

$M_{S\text{-}e}$ = 1294.7731 kip-ft and $M_{S\text{-}i}$ = 1118.2235 kip-ft

The stress under service load at the bottom flange can be derived from the following equation:

$$f_s = \frac{M_{beam}}{S_b} + \frac{M_{deck}}{S_{b3n}} + \frac{M_{bar}}{S_{b3n}} + \frac{M_{FW}}{S_{b3n}} + \frac{M_{truck} I_m DF}{S_{bn}} + \frac{M_{lane}}{S_{bn}} \tag{6}$$

$f_{s\_i} = 27.64 ksi = 67.42\% \times F_y$

$f_{s\_e} = 31.06 ksi = 75.75\% \times F_y$

The bottom flange stress under the service load calculated using LRFD specifications are beyond the 55 percent proportion of yield strength that is usually regarded as limited stress under a service load. To estimate the ultimate flexural capability, a full plastic analysis method was used, and the location of the plastic axis must be determined using the following equation:

$$c = \frac{A_s\, F_y}{0.85 f_c S} \tag{7}$$

where,

A_s = area of reinforcement,

F_y = yield strength of steel, and

f_c = concrete strength.

If $c \leq 8in$, the thickness of the deck, the plastic axis is located in the deck; otherwise, it is located in the steel beam. The flexural moment at the ultimate state of the steel I-beam girder can be derived from the balance equations. For exterior girders:

$$cc_e = \frac{A\, F_y}{0.85 f_c \times 84} = 7.45\ in \tag{8}$$

The plastic axis is located in the deck. The nominal moment is:

$$M_{n\_e} = A\, F_y \times \left(\frac{d}{2} + \frac{c}{2}\right) = 707.493\ kip\ ft \tag{9}$$

The nominal moment for interior-exterior girders is derived the same way. Unlike exterior girders, the plastic axis of the interior-exterior girder is located in the bottom surface of the top flange. The nominal moment is:

$$M_{n\_i} = P_c\left(4 + \frac{7}{8}\right) + \frac{7}{8} \times 11\left(d - \frac{7}{8}\right)F_y + \frac{1}{2} \times \frac{5}{8}\left(d - 2 \times \frac{7}{8}\right)^2 F_y \tag{10}$$

$$M_{n\_i} = 2621.349\ kip\ ft$$

Compared to the total moment at the ultimate state, the flexural capability is sufficient.

Mechanical Flexural Capacity Analysis of Girders Strengthened with FRP Materials

To estimate the flexural capacity of reinforced concrete girders strengthened with prestressed CFRP laminates, three types of failure modes must be identified: tension failure, i.e., rupture of CFRP plate prior the crushing of concrete in compression; debonding failure, i.e., force in the prestressed CFRP plate could not be sustained by the concrete substrate, which results in the CFRP plate debonding prior to the concrete crushing; and, compression failure, i.e., crushing of concrete in compression prior to the rupture or debonding of CFRP plate. These three types of failure modes control the ultimate capacity in RC beams. The boundary to distinguish tension, debonding failure, and compression failure is its balance state. At the balance state, the tensile strain in the prestressed CFRP plate equals the tensile strain limitation$[\mathcal{E}_{pfu}]$, with the compression concrete crushed at the same time.

Strengthened with Bonded Prestressed FRP Laminates

Bonded, non-prestressed beams strengthened with one layer of FRP laminate tend to fail due to brittle intermediate crack-induced debonding from the mid-to-end when the strain of the laminates reached about 6500-7000μ, while beams strengthened with more laminates tend to plate-end debonding when the CFRP plate strain reached about 5200μ. It was concluded that the strengthening efficiency of the member strengthened with one laminate is better than that of the member strengthened with two or more laminates with FRP anchored at the two ends of the member *[16]*.

Badawi and Soudki and Xue et al. proposed an analytical model and flexural capacity prediction formulas for reinforced concrete beams strengthened with prestressed NSM CFRP rods and bonding CFRP plates, respectively *[9,13]*. They both introduced fundamental assumptions relating to flexure used in calculating the nominal flexural strength for reinforced concrete girders. It seems that these assumptions are still applicable in flexural capacity estimation for reinforced concrete girders strengthened with prestressed CFRP materials:

1. A cross section that was plane before loading remains plane under a load. The strain in the reinforcement and concrete are directly proportional to the distance from the neutral axis.

2. The bending stress at any point depends on the strain at the point in a manner given by the stress-strain diagram of the material.

3. The tensile strength of concrete is ignored.

The analysis models are based on force equilibrium and strain compatibility. Xue et al. introduced compressive stress of concrete corresponding to a given strain, f_c, as *[13,30]:*

$$f_c = \begin{cases} f_c'\left[\dfrac{2\mathcal{E}_c}{\mathcal{E}_0} - \left(\dfrac{\mathcal{E}_c}{\mathcal{E}_0}\right)^2\right] & if\ 0 \le \mathcal{E}_c \le \mathcal{E}_0 \\ f_c'\left[1 - \dfrac{0.15}{0.004 - \mathcal{E}_0}(\mathcal{E}_c - \mathcal{E}_0)\right] & if\ \mathcal{E}_0 \le \mathcal{E}_c \le 0.003 \end{cases} \quad (11)$$

where, f_c' is the cylinder compressive strength of concrete; $\mathcal{E}_c$ is the compressive concrete strain; and $\mathcal{E}_0$ is the compressive strain in concrete at the peak stress. In this calculation, the concrete is about to crush when the ultimate compressive strain reaches 0.003 for normal-density concretes. Reinforcing steel is assumed to behave in an elastic-perfectly plastic response, and the FRP plate has a linear elastic stress–strain relationship up to failure. The shear deformation within the adhesive layer is neglected since the adhesive layer is very thin with slight variations in its thickness. Figures 19, 20, and 21 show the diagram of tension, debonding, compression failure modes, and the balanced state of a concrete section.

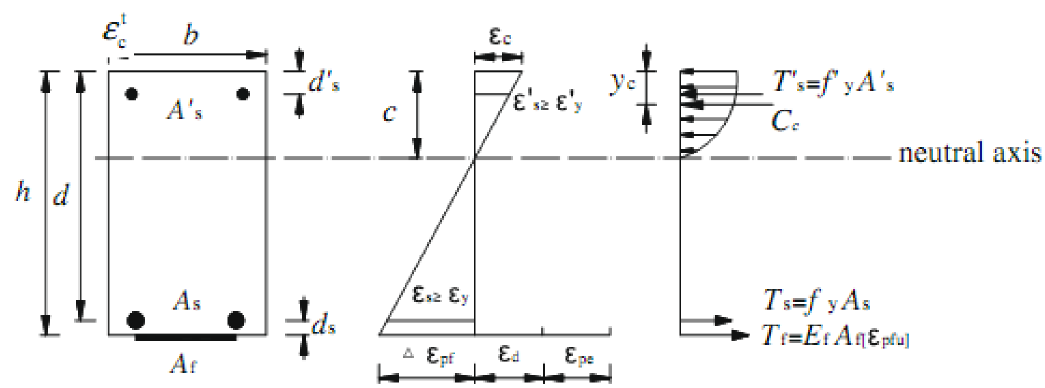

Figure 19
Internal strain and stress distribution for the strengthened section under the debonding failure or tension failure

[adopted from Xue et al. (2010)]

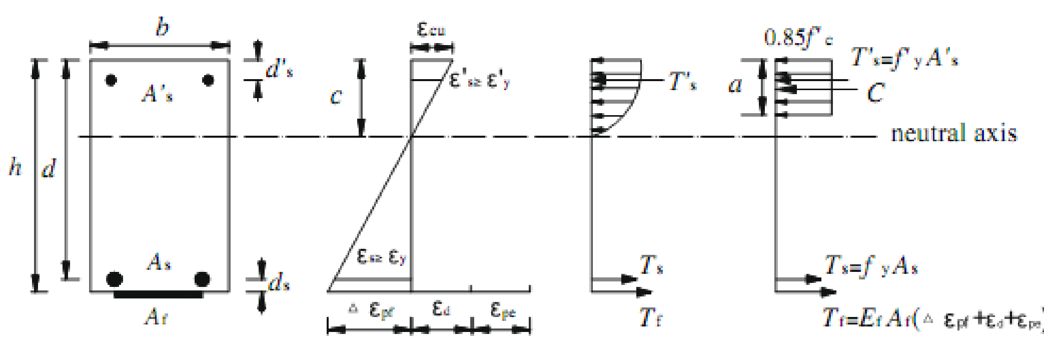

Figure 20
Internal strain and stress distribution for the strengthened section under the compression failure

[adopted from Xue et al. (2010)]

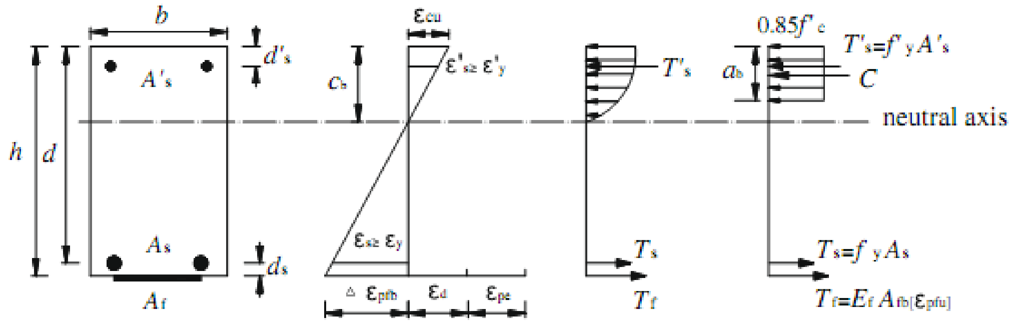

Figure 21
Internal strain and stress distribution for the strengthened section with a balanced reinforcement ratio
[adopted from Xue et al. (2010)]

After the decompression state, the extreme precompressed fiber reaches zero strain due to the additional strain in the prestressed CFRP laminate, ε_d. The prestressed concrete beam is treated as the corresponding nonprestressed beam in the capacity analysis. The tensile strain limitation, $\mathcal{E}_{pfu}$, the ultimate strain increase in the CFRP laminate after decompression, is proposed for predicting the maximum tensile strain level in the prestressed CFRP laminate under the debonding failure or tension failure.

$$[\mathcal{E}_{pfu}] = \begin{cases} \mathcal{E}_{pe} + \mathcal{E}_d + \kappa_m \mathcal{E}_{pfu} < \mathcal{E}_{pfu} & if\ \mathcal{E}_{pe} + \mathcal{E}_d + \kappa_m \mathcal{E}_{pfu} < \mathcal{E}_{pfu} \\ & (debonding\ failure) \\ \mathcal{E}_{pfu} & if\ \mathcal{E}_{pe} + \mathcal{E}_d + \kappa_m \mathcal{E}_{pfu} \geq \mathcal{E}_{pfu} \\ & (tension\ failure) \end{cases} \tag{12}$$

In equation (12), $\kappa_m \mathcal{E}_{pfu}$ refers to the strain increase limitation for the prestressed CFRP laminate, which can be determined by following equation suggested by ACI 440.2R-02 to prevent the debonding failure of non prestressed CFRP laminate:

$$\kappa_m \mathcal{E}_{pfu} = \begin{cases} \dfrac{1}{60}\left(1 - \dfrac{nE_f t_f}{360000}\right) \leq 0.9\mathcal{E}_{pfu} & for\ \ nE_f t_f \leq 180000 \\ \dfrac{1}{60}\left(\dfrac{90000}{nE_f t_f}\right) \leq 0.9\mathcal{E}_{pfu} & for\ \ nE_f t_f > 180000 \end{cases} \tag{13}$$

where, κ_m is the reduction factor; n is the number of plies of the CFRP laminate at the location along the length of the member where the moment is being calculated; E_f is the tension modulus of elasticity of CFRP laminate (MPa); and t_f is the thickness of CFRP laminate (mm). The identification of failure mode based on strain compatibility and plane strain assumption:

$$\frac{\mathcal{E}_{cu}}{\Delta\mathcal{E}_{pfb}} = \frac{c_b}{h - c_b} = \frac{a_b/\beta_1}{h - a_b/\beta_1} \tag{14}$$

from which the a_b is determined. The balanced CFRP reinforcement ratio of the strengthened section is implied from equation (15):

$$\rho_{fb} = \frac{A_{fb}}{bd} = \frac{0.85 f_c' b a_b - f_y A_s + f_y' A_s'}{bd E_f \mathcal{E}_{pfu}} \tag{15}$$

The concrete crushing failure of the compression zone occurs when the CFRP reinforcement ratio, $\rho_f = A_f/bd$, exceeds ρ_{fb} or the depth of equivalent rectangular concrete stress block a exceeds a_b; the strengthened beams will fail by concrete crushing in the compression zone; otherwise, the debonding failure or tension failure occurs in the strengthened beam.

For compression failure, based on the assumption of liner strain distribution, the following equation can be obtained:

$$\frac{\mathcal{E}_{cu}}{\Delta\mathcal{E}_{pf}} = \frac{c}{h - c} = \frac{a/\beta_1}{h - a/\beta_1} \tag{16}$$

where c is the depth of neutral axis; a is the depth of the equivalent rectangular concrete stress block; and $\Delta\mathcal{E}_{pf}$ is the ultimate strain increment in the prestressed CFRP materials for the strengthened beam. The equilibrium of internal forces leads to the following equation:

$$0.85 f_c' b \beta_1 c + f_y' A_s' = f_y A_s + E_f A_f \left(\mathcal{E}_{pe} + \mathcal{E}_d + \Delta\mathcal{E}_{pf}\right) \tag{17}$$

and the corresponding nominal flexural strength under compression failure can be given by summing the moments about the centroid of the concrete compressive force:

$$\begin{aligned} M_n = {} & f_y A_s \left(d - \frac{a}{2}\right) + f_y' A_s' \left(\frac{a}{2} - d_s'\right) \\ & + E_f A_f \left(\mathcal{E}_{pe} + \mathcal{E}_d + \Delta\mathcal{E}_{pf}\right)\left(h - \frac{a}{2}\right) \end{aligned} \tag{18}$$

When the tension of debonding failure occurs, the compression strain in the extreme fiber of concrete, $\mathcal{E}_c^t$, is derived from the following equation obtained based on the plane strain assumption:

$$\mathcal{E}_c^t = \frac{c}{h-c}\Delta\mathcal{E}_{pf} \tag{19}$$

The concrete compression force is solved by integration of the concrete stress within the range of the compression zone.

$$C_c = \int_0^c f_c' bc\left[\frac{2\mathcal{E}_c^t y}{\mathcal{E}_0 c} - \frac{(\mathcal{E}_c^t y/c)^2}{\mathcal{E}_0}\right]dy = f_c' bc\frac{\mathcal{E}_c^t}{\mathcal{E}_0}\left(1 - \frac{\mathcal{E}_c^t}{3\mathcal{E}_0}\right) \tag{20}$$

The equilibrium of internal forces leads to the following equation:

$$C_c + f_y' A_s' = f_y A_s + E_f A_f\left(\mathcal{E}_{pe} + \mathcal{E}_d + \Delta\mathcal{E}_{pf}\right) \tag{21}$$

The length of the range of the compression zone is solved using equation (22). The distance from the top concrete fiber to the centroid of the concrete compressive force is y_c:

$$y_c = \frac{\int_0^c f_c' bc\left[\frac{2\mathcal{E}_c^t y}{\mathcal{E}_0 c} - \frac{(\mathcal{E}_c^t y/c)^2}{\mathcal{E}_0}\right](c-y)dy}{C_c} = \frac{c(\mathcal{E}_c^t - 4\mathcal{E}_0)}{4(\mathcal{E}_c^t - 3\mathcal{E}_0)} \tag{22}$$

The corresponding nominal flexural strength is computed by summing moments about the centroid of the concrete compressive force:

$$M_n = f_y A_s(d - y_c) + f_y' A_s'(y_c - d_s) + E_f\left[\mathcal{E}_{pfu}\right]A_f(h - y_c) \tag{23}$$

Strengthened with External Unbonded Prestressed FRP Materials

ACI 440.4R-04 proposed a method to calculate the ultimate nominal flexural capability of prestressing concrete structures with FRP tendons. For unbounded prestressed members, the stress in the prestressing tendons at failure of the beam must be determined using the following relation:

$$f_p = f_{pe} + \Delta f_p \tag{24}$$

where, f_{pe} is the effective prestress in the tendon when the beam carriers only the dead load after the prestress losses have occurred, and Δf_p is the stress increase above f_{pe} due to any additional applied load. The Δf_p can be derived using strain compatibility as if the tendon were bonded and applies a strain reduction factor Ω to account for the fact that the tendons were unbonded. Assuming linear elastic behavior of the tendon, the change in stress Δf_p in the unbounded tendon is given by:

$$\Delta f_p = \Omega_u E_p \varepsilon_{cu} \left(\frac{d_p}{c_u} - 1\right) \tag{25}$$

where, ε_{cu} is the strain in the extreme compression fiber at the ultimate state, and c_u is the depth of the neutral axis at the ultimate state. According to Alkhairi and Naaman, the strain reduction coefficient at ultimate, Ω_u can be determined by *[31]*:

$$\Omega_u = \frac{2.6}{(L/d_p)} \quad \text{(for two} - \text{one point loading)} \tag{26}$$

$$\Omega_u = \frac{5.4}{(L/d_p)} \quad \text{(for two} - \text{point or uniform loading)} \tag{27}$$

For design purposes, the above formulas were emended as

$$\Omega_u = \frac{1.5}{\left(\frac{L}{d_p}\right)} \quad \text{(for one point loading)} \tag{28}$$

$$\Omega_u = \frac{3.0}{(L/d_p)} \quad \text{(for two} - \text{point or uniform loading)} \tag{29}$$

ACI 440.4R.-04 proposed a method to estimate stress in an external unbonded prestressed at the ultimate state. According to Aravinthan et al., equations for the strain reduction coefficient Ω_u used to predict the behavior at the ultimate state of beams with external prestressing or a combination of internal and external prestressing, are as follows *[32]*:

$$\Omega_u = \frac{0.21}{(L/d_p)} + 0.04\left(\frac{A_{p\,int}}{A_{p\,tot}}\right) + 0.04 \tag{30}$$

for one-point loading and

$$\Omega_u = \frac{0.231}{(L/d_p)} + 0.21\left(\frac{A_{p\,int}}{A_{p\,tot}}\right) + 0.046 \tag{31}$$

for three-point loading where $A_{p\,int}$ is the area of the internal prestressed reinforcement, and $A_{p\,tot}$ is the total area of internal and external prestressed reinforcement.

DISCUSSION OF RESULTS

Rehabilitation with External Bonded Prestressed CFRP Materials

CFRP Material Mechanical Properties and Anchorage System

To rehabilitate the girders with external post-tensioning materials is an effective way to enhance girders’ flexural capability. In the tentative design, the CFRP laminates were selected to serve as prestressed reinforcements. The CFRP laminates were prestressed before they are bonded to the bottom surfaces of the girders. All the construction can be conducted with specially designed machines. As discovered previously, several properties, such as high strength, relative high modulus of elasticity, excellent corrosion and fatigue resistance make CFRP material one of the best choices of external post-tensioning tendons. Sika CarboDur is a pultruded carbon fiber reinforced polymer (CFRP) laminate designed for strengthening concrete, timber, and masonry structures, and its mechanical properties are shown in Table 10.

Table 10
Properties of Sika CarboDur laminate

<table>
<tr><td rowspan="2">Tensile Strength</td><td>Mean value</td><td>4.49E5 psi</td><td>3100 Mpa</td></tr>
<tr><td>Design value</td><td>4.06E5 psi</td><td>2800 Mpa</td></tr>
<tr><td rowspan="2">Modulus of elasticity</td><td>Mean value</td><td>23.9E6 psi</td><td>165000 Mpa</td></tr>
<tr><td>Design value</td><td>23.2E6 psi</td><td>160000 Mpa</td></tr>
<tr><td colspan="2">Elongation at break</td><td colspan="2">1.69%</td></tr>
<tr><td colspan="2">Design Strain</td><td colspan="2">0.85%</td></tr>
<tr><td colspan="2">Thickness</td><td>0.047 in</td><td>1.2 mm</td></tr>
<tr><td colspan="2">Temperature resistance</td><td>>300 °F</td><td>>150 °C</td></tr>
<tr><td colspan="2">Fiber volumetric content</td><td colspan="2">> 68%</td></tr>
<tr><td colspan="2">Density</td><td>0.058 lbs/c.in</td><td>1.60 g/c.cm</td></tr>
</table>

Sika CarboDur, carbon fiber laminate for structural strengthening, is widely used in the civil engineering field. Commercial CFRP products are available in forms of laminates and bars. Table 11 presents mechanical properties of commercial products of Sika CarboDur laminates. Because long-term exposure to various type of environments can reduce the tensile properties, creep-rupture, and fatigue endurance of FRP laminates, the material properties used in design equations should be reduced based on the environmental exposure condition. The environmental-reduction factor, 0.85, is induced from ACI 440.2R-2 Table 8.1.Thus, the design value of Sika CarboDur laminate, f_{pu} is reduced to 3.451x10^5 psi.

Table 11
Mechanical properties of Sika CarboDur commercial products

Product	Thickness mil / (mm)	Width in. / (mm)	Cross Section Area sq.in. / (mm²)	Tensile Strength lb. / (kN)
Type S 512	47.2 / (1.2)	1.97/ (50)	0.093 / (60)	37.8E3 / (168)
Type S 812	47.2 / (1.2)	3.15 / (80)	0.149 / (96)	60.4E3 / (269)
Type S 1012	47.2 / (1.2)	3.94 / (100)	0.186 / (120)	75.5E3 / (336)

Laminates and anchorages are usually provided together by manufacturers. The shape of stressing anchorage *Type Es* and fixed anchorage type *Ef* are shown in Figures 22 and 23.

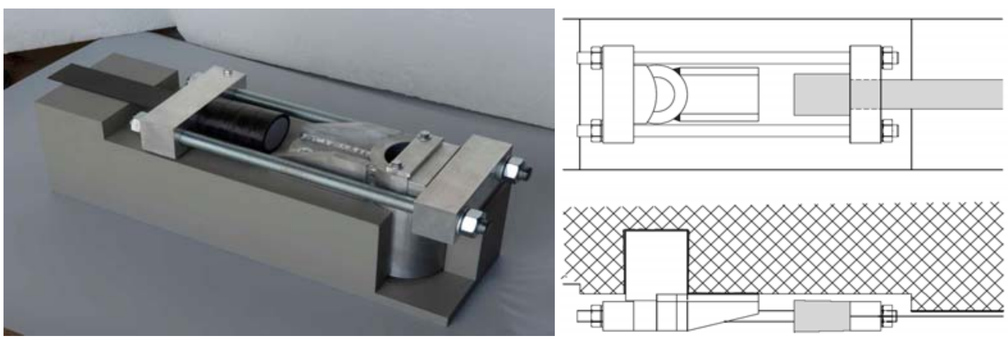

Figure 22
Stressing anchorage: Type Es

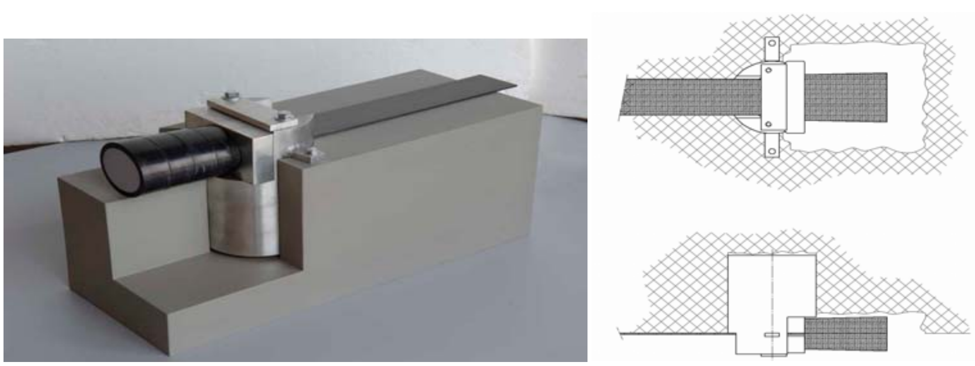

Figure 23
Fix anchorage: Type Ef

Concrete Span

Exterior Concrete Girders Flexural Capacity

In the tentative design, two S 1012 CFRP laminates with dimensions of 3.94 in. x 0.047 in. (100 mm x 1.2 mm) were applied to restore the flexural capacity of both the exterior girders with a total section area of 0.372 in^2. The initial prestress applied to the CFRP laminates is 0.50 x 0.85 f_{pu}. Because the information of stress loss is limited, in this calculation, the stress loss is assumed to be 15 percent.

The effective stress in the CFRP laminates after all losses is:

$$f_{pe} = 0.50\, f_{pu}(1 - 0.15) = 146.667 ksi \tag{32}$$

and correspondingly, the effective strain is:

$$\mathcal{E}_{pe} = \frac{f_{pe}}{E_f} = 6.322 \times 10^{-3} \tag{33}$$

where, f_{pu} is the nominal tensile strength of the prestressed CFRP laminate; and E_f is the tension modulus of elasticity of the CFRP laminate. In this calculation, for the external girder, the additional strain in the prestressed CFRP laminate, $\mathcal{E}_d$, leading to the state of decompression is:

$$\mathcal{E}_d = \frac{h - c}{E_c c}\left(\frac{f_{pe}A_f}{A_e} - \frac{f_{pe}A_f(h - c)}{\frac{I_e}{c}}\right) = 7.210 \times 10^{-5} \tag{32}$$

The strain increase limitation for the prestressed CFRP laminates is:

$$\kappa_m \mathcal{E}_{pfu} = \frac{1}{60}\left(\frac{90000}{nE_f t_f}\right) = 7.8125 \times 10^{-3} \tag{34}$$

thus, the strain increase for the prestressed CFRP laminates is equal to $\kappa_m \mathcal{E}_{pfu}$.

From equation (14), we have:

$$c_b = \frac{\mathcal{E}_{cu} h}{\mathcal{E}_{cu} + \Delta\mathcal{E}_{pfb}} = 8.879\ in \tag{35}$$

The depth of the corresponding concrete compressing block is:

$$a_b = 0.85c_b = 7.547\ in \tag{36}$$

The balanced CFRP reinforcement ratio of the strengthened section is calculated from equation (15):

$$\rho_{fb} = \frac{A_{fb}}{bd} = \frac{0.85f_c'ba_b - f_yA_s + f_y'A_s'}{bdE_f\mathcal{E}_{pfu}} = 1.384 \times 10^{-3} \tag{37}$$

The failure mode is identified using equation (15). Since $\rho_f < \rho_{fb}$, it is confirmed that the exterior girders strengthened with prestressed CFRP laminates will experience tension or debonding failure.

The compressive strain in concrete at the peak stress is:

$$\mathcal{E}_0 = 2\frac{f_c}{E_c} = 1.922 \times 10^{-3} \tag{38}$$

The compressive concrete strain is derived using:

$$\mathcal{E}_c = \frac{c}{h-c}\Delta\mathcal{E}_{pfb} = 1.803 \times 10^{-3} \tag{39}$$

The total strain of CFRP laminates is:

$$\mathcal{E}_{pfu} = \mathcal{E}_{pe} + \mathcal{E}_d + \kappa_m\mathcal{E}_{pfu} = 0.0143 \tag{40}$$

By solving equilibrium equations, the depth of the concrete compression zone is $4.186\ in$.

The nominal flexural capacity of the exterior concrete girders rehabilitated with prestressed CFRP laminates is:

$$M_{n\_e} = f_yA_s(h_s - y_c) + \mathcal{E}_{pfu}E_fA_f(h - y_c) = 1140.7\ kip\ ft \tag{41}$$

Multiplying the factor 0.9, we have:

$$0.9M_{n\_e} = 1026.2\ kip\ ft \approx M_{T\_e} = 1048.734\ kip\ ft \tag{42}$$

Therefore, the flexural capacity after rehabilitation satisfies the requirement.

The CFRP laminates share the load effects of future wearing, truck, and lane load. For the service state, all the load combination factors are 1.0

$$M_{s\_e} = F_w + M_{truk} + M_{lane} = 360.78\ kip\ ft \tag{43}$$

Stress in the CFRP laminates is:

$$f_s = \frac{M_{s\_e}}{S_{b\_e}} + f_e = 0.522 f_u < 0.55 f_u \tag{44}$$

The stress in the CFRP laminates under service state satisfies the requirement.

Interior-Exterior Concrete Girders Flexural Capacity

Similar to the exterior girders, two S 1012 CFRP laminates with dimensions of 3.94 in. x 0.047 in. (100 mm x 1.2 mm) were applied to restore the flexural capacity of both the interior-exterior girders with a total section area of 0.372 in^2.The initial prestress applied to the CFRP laminates is $0.20 \times 0.85 f_{pu}$. Because the information of stress loss is limited, in this calculation, the stress loss is assumed to be 15 percent.

The effective stress in the CFRP laminates after all losses is:

$$f_{pe} = 0.50\, f_{pu}(1 - 0.15) = 146.667 ksi \tag{45}$$

and correspondingly, the effective strain is:

$$\frac{\mathcal{E}_{pe} = f_{pe}}{E_f} = 6.322 \times 10^{-3} \tag{46}$$

where, f_{pu} is the nominal tensile strength of the prestressed CFRP laminate; and E_f is the tension modulus of elasticity of the CFRP laminate. In this calculation, for the interior-external girder, the additional strain in the prestressed CFRP laminate, ϵ_d, leading to the state of decompression is:

$$\mathcal{E}_d = \frac{h - c}{E_c c}\left(\frac{f_{pe} A_f}{A_e} - \frac{f_{pe} A_f (h - c)}{\frac{I_e}{c}}\right) = 7.813 \times 10^{-5} \tag{47}$$

The strain increase limitation for the prestressed CFRP laminates is:

$$\kappa_m \mathcal{E}_{pfu} = \frac{1}{60}\left(\frac{90000}{n E_f t_f}\right) = 7.8125 \times 10^{-3} \tag{48}$$

thus, strain increase for the prestressed CFRP laminates is equal to $k_m \epsilon_{pfu}$.

From equation (14), we have:

$$c_b = \frac{\mathcal{E}_{cu} h}{\mathcal{E}_{cu} + \Delta\mathcal{E}_{pfb}} = 8.879\ in \tag{49}$$

The depth of the corresponding concrete compression block is:

$$a_b = 0.85 c_b = 7.547\ in \tag{50}$$

The balanced CFRP reinforcement ratio of strengthened section is implied from equation (51)

$$\rho_{fb} = \frac{A_{fb}}{bd} = \frac{0.85 f_c' b a_b - f_y A_s + f_y' A_s'}{bd E_f \mathcal{E}_{pfu}} = 1.35 \times 10^{-3} \tag{51}$$

The failure mode is identified using equation (15). Since $\rho_f < \rho_{fb}$, it is confirmed that the exterior girders strengthened with prestressed CFRP laminates will experience tension or debonding failure.

The compressive strain in concrete at the peak stress is:

$$\mathcal{E}_0 = 2\frac{f_c}{E_c} = 1.922 \times 10^{-3} \tag{52}$$

The compressive concrete strain is derived using:

$$\mathcal{E}_c = \frac{c}{h-c} \Delta\mathcal{E}_{pfb} = 1.264 \times 10^{-3} \tag{53}$$

The total strain of CFRP laminates is:

$$\mathcal{E}_{pfu} = \mathcal{E}_{pe} + \mathcal{E}_d + \kappa_m \mathcal{E}_{pfu} = 0.0154 \tag{54}$$

By solving equilibrium equations, the depth of the concrete compression zone is 4.456 in.

The nominal flexural capacity of the interior-exterior concrete girders rehabilitated with prestressed CFRP laminates is:

$$M_{n\_i} = f_y A_s (h_s - y_c) + \mathcal{E}_{pfu} E_f A_f (h - y_c) = 1101.74\ kip\ ft \tag{55}$$

Multiplying the factor 0.9 we have:

$$0.9 M_{n\_i} = 1023.966\ kip\ ft > M_{T\_e} = 991.566\ kip\ ft \tag{56}$$

Therefore, the flexural capacity after rehabilitation satisfies the requirement.

The CFRP laminates share the load effects of future wearing, truck and lane load. For the service state, all the load combination factors are 1.0.

$$M_{s\_i} = F_w + M_{truk} + M_{lane} = 360.78\ kip\ ft \tag{57}$$

Stress in the CFRP laminates is:

$$f_s = \frac{M_{s\_i}}{S_{b\_i}} + f_e = 0.523 f_u < 0.55 f_u \tag{58}$$

The stress in the CFRP laminates under service state satisfies the requirement.

Steel Span

In order to reduce the steel girder stress under the service load, the steel I-beam girder can also be rehabilitated with externally prestressed CFRP laminates. The stress under service load can be reduced to 55 percent of the steel yield strength f_y. A S1024 CFRP laminate was installed in each girder, and they are located at the bottom of the steel girder. The initial prestress applied to the CFRP laminates are assumed to be 0.45 f_{pfu} and the stress loss is assumed to be 15 percent. The effective stress in the CFRP laminates after all losses is:

$$f_{pe} = 0.45\ f_{pfu}(1 - 0.15) = 155.25\ ksi \tag{59}$$

The steel girder stress under service is obtained from following equation:

$$f_s = \frac{M_{beam}}{S_b} + \frac{M_{deck}}{S_{b3n}} + \frac{M_{bar}}{S_{b3n}} + \frac{M_{FW}}{S_{b3n}} + \frac{M_{truck} I_m DF}{S_{bn}} + \frac{M_{lane} I_m DF}{S_{bn}} - \frac{T_{ten}}{A_{c3n}} - \frac{T_{ten} y_{b3n}}{S_{b3n}} \tag{60}$$

For exterior girders, we have $f_{s\_e} = 22.271\ ksi = 0.543 f_y$ and for interior-exterior girders we have $f_{s\_i} = 21.138\ ksi = 0.516 f_y$

Both of them are smaller than $0.55 f_y$. The tension stress in the CFRP laminates under service traffic load is obtained from following equation:

$$f_{pf} = \frac{M_{FW}}{S_{b3n}} + \frac{M_{truck} I_m DF}{S_{bn}} + \frac{M_{lane} I_m DF}{S_{bn}} + f_{pe} \tag{61}$$

For exterior girders, we have $f_{pf\_e} = 171.235\ ksi = 0.496 f_{fpu}$ and for interior-exterior girders, we have $f_{pf\_i} = 169.314\ ksi = 0.491 f_{fpu}$. Both of them are smaller than $0.55 f_{pfu}$.

3-D Finite Element Analysis

Two 3-D finite element analysis models were developed for both the concrete approach span and main crossing steel span with ANSYS (Release 13.0).

Finite Element Type

For the concrete span, both the concrete deck and the concrete girder were simulated with SOLID45 elements. SOLID45 was used for the 3-D modeling of solid structures. The element was defined by eight nodes having three degrees of freedom at each node: translations in the nodal x, y, and z directions. For the steel girder span, the concrete deck is simulated with SOLID 73, and the steel girder flanges and web were simulated with SHELL63 elements. Unlike SOLID45, besides three translation freedoms at each node, each node of SOLID73 has additional three degrees of rotation freedom. SHELL63 has both bending and membrane capabilities. Both in-plane and normal loads are permitted. The element has six degrees of freedom at each node: translations in the nodal x, y, and z directions and rotations about the nodal x, y, and z-axes. Stress stiffening and large deflection capabilities are included. A consistent tangent stiffness matrix option is available for use in large deflection (finite rotation) analyses. The top flange and bottom deck surface were connected with stiff arms, which were simulated with BEAM 4, a uniaxial element with tension, compression, torsion, and bending capabilities. BEAM 4 elements have six degrees of freedom at each node: translations in the nodal x, y, and z directions and rotations about the nodal x, y, and z axes. With the connection of the stiff arms between the concrete deck and steel girders, the main cross section was considered as a full composite section, without relative displacement between these two materials. To ensure the side stability of the slender web, the contribution of the diaphragms was realized by coupling the transverse deformation of the web at the diaphragms position, one at the mid-span, and two at the location 1 ft. (0.30 m) away from the two ends.

Load Combination

The dead load and live load were included in the models. For the purpose of simplicity, the dead load of the wearing surface, diaphragms, and barrier were ignored in the preliminary analysis. Two HL-93 trucks were put in the worst position side–by-side along the longitudinal direction. The setup of the two trucks is shown in Figures 24 and 25. Two load combination cases, considering the strength limit state and service limit state, were calculated using different combination factors. For the service limit state, combination factors for dead load and live load are 1.0; for the strength limit state, the factors are 1.25 and 1.75, respectively. For both load combination cases, the live load impact factor, 1.33, was included.

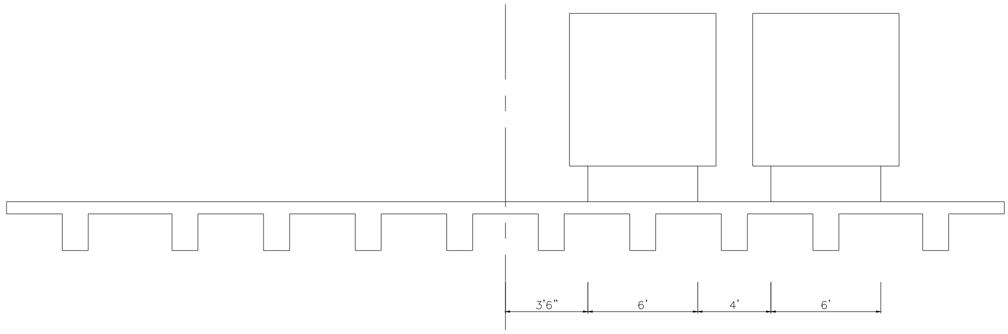

Figure 24
Truck position in concrete span

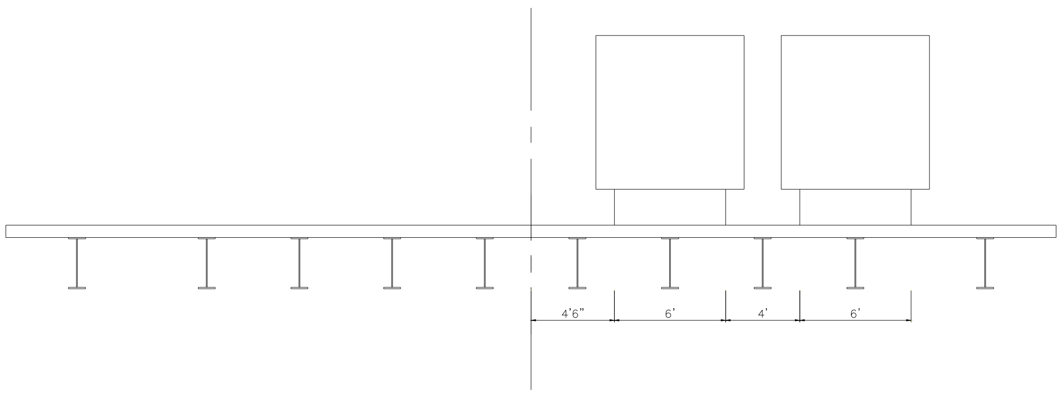

Figure 25
Truck position in steel span

3-D Finite Element Analysis Result

The external prestressed CFRP laminates were simulated with external force for exterior and interior-exterior girders applied at the anchorage positions. The prestressed force is equal to the effective prestress force when the CFRP materials were applied on the girders, which was used in the tentative design mentioned previously. This simplification does not take the consideration of the increments in the prestress force when the live load is applied on the girders, thus the improvement of the performance of the girders rehabilitated with prestressed CFRP laminates is conservatively underestimated in the finite element model.

Tables 12 and 13 list the mid-span deflection and bottom fiber stress of concrete girders and steel girders, respectively. The deformation of the entire bridge and the longitudinal stress among the bridge under live load, only in both service limit state and strength limit state, are shown in Figures 26 to 37.

The deflection due to the truckload was 0.207 in. (0.005 m) for the concrete span and 1.347 in. (0.03 m) for the steel span. This deflection in steel span exceeded the requirement of

L/800. After the rehabilitation, the deflection reduced to 0.157 in. (0.004 m) and 1.009 in. (0.03 m), respectively. It was shown that the rehabilitation with prestressed CFRP reduced the bottom stress by 5 percent to 10 percent. One should notice that the stress calculated with the 3-D finite element model is much smaller than that calculated from AASHTO *[33]*. For the steel span, the result was sensitive to the connections between the shell elements and solid elements. It is recommended a field test is needed to improve the accuracy of the finite element models. In addition, since the stress increments in the CFRP are ignored, the realistic contribution of the CFRP laminate is greater than the calculation result.

Table 12
Concrete girder mid-span stress and deflection

	before rehabilitation			after rehabilitation		
	live load	service limit state	Strength limit state	live load	service limit state	Strength limit state
stress (psi)	611.8	1235.9	1850.8	402	1026.2	1641.1
deflection (in.)	0.2066	0.4177	0.6242	0.1571	0.3665	0.5693

Table 13
Steel girder mid-span stress and deflection

	before rehabilitation			after rehabilitation		
	live load	service limit state	Strength limit state	live load	service limit state	Strength limit state
stress (psi)	2672.1	5522.5	8239.2	2233.4	5083.9	7790.1
deflection (in.)	1.347	3.1016	4.5475	1.009	2.7326	4.1787

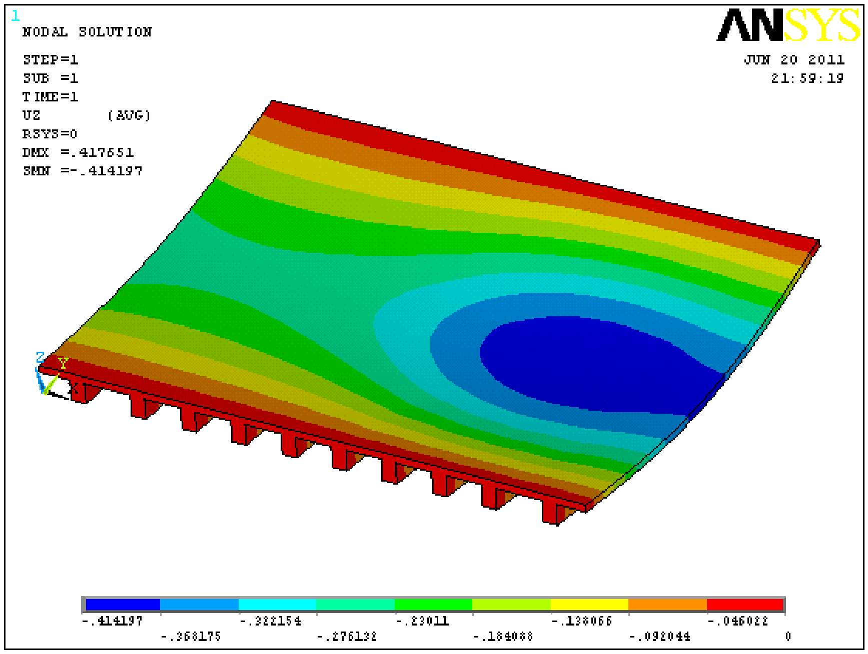

Figure 26
Concrete span deformation under service limit state before rehabilitation

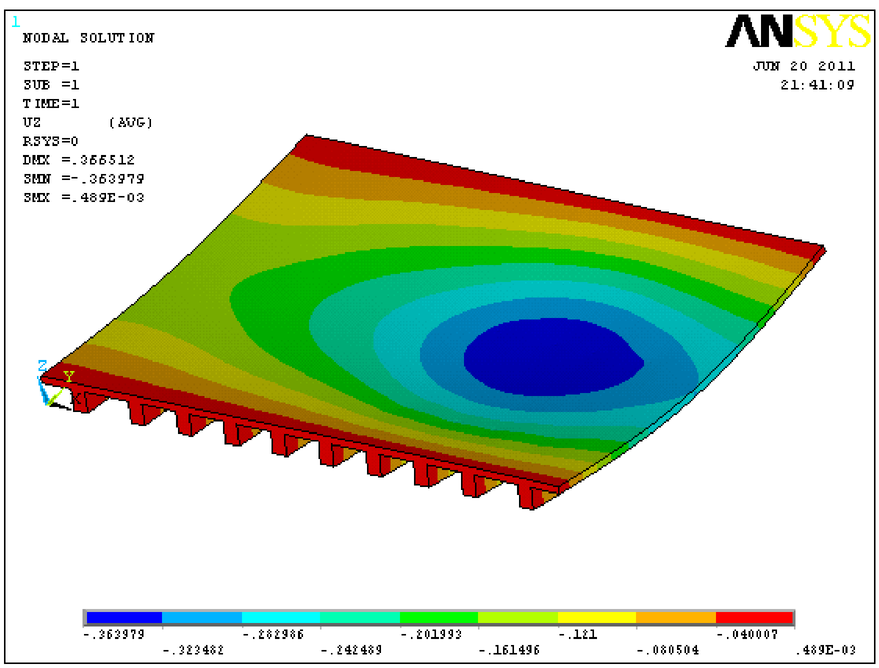

Figure 27
Concrete span deformation under service limit state after rehabilitation

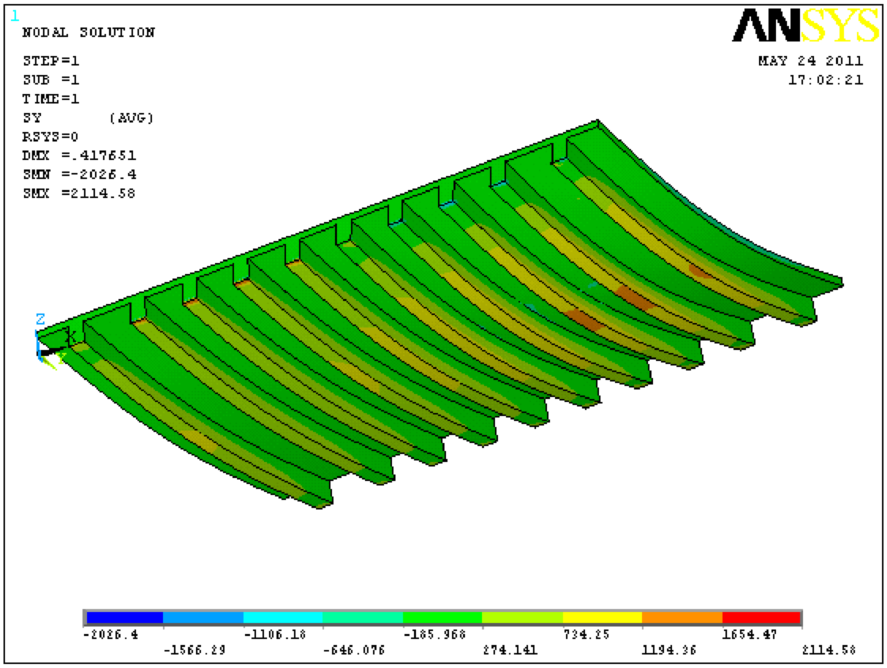

Figure 28
Concrete girders longitudinal stress under service limit state before rehabilitation

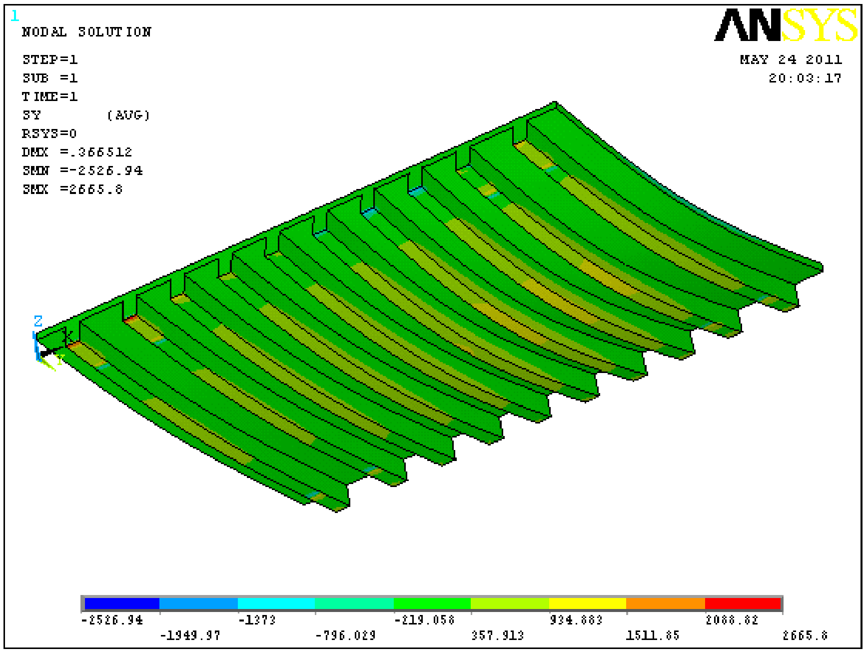

Figure 29
Concrete girders longitudinal stress under service limit state after rehabilitation

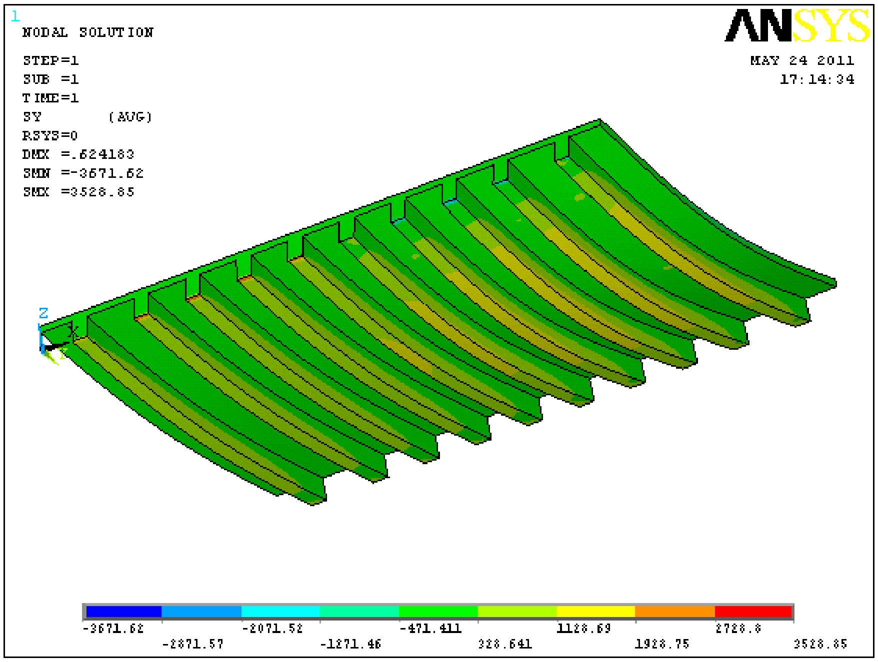

Figure 30
Concrete girders longitudinal stress under strength limit state before rehabilitation

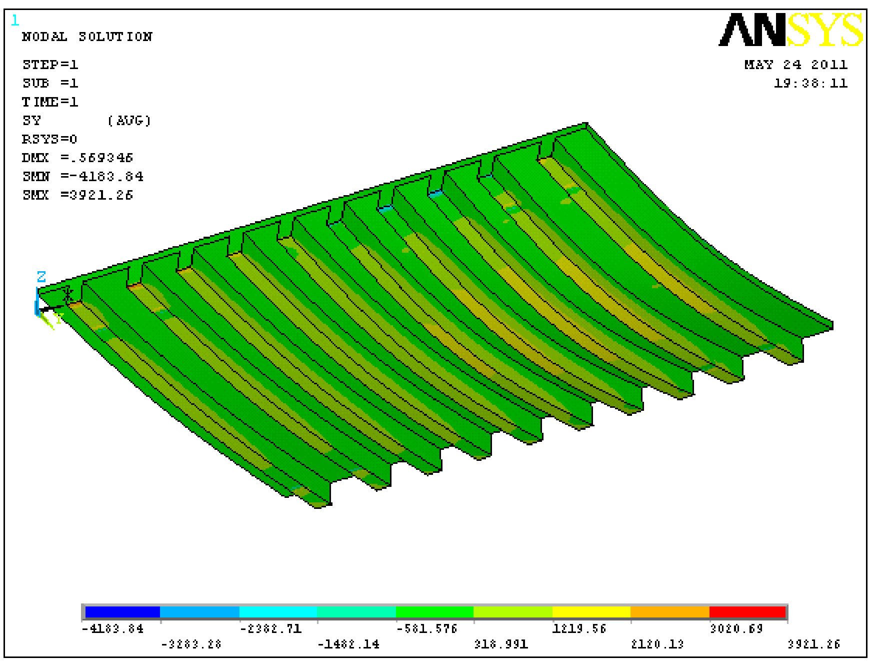

Figure 31
Concrete girders longitudinal stress under strength limit state after rehabilitation

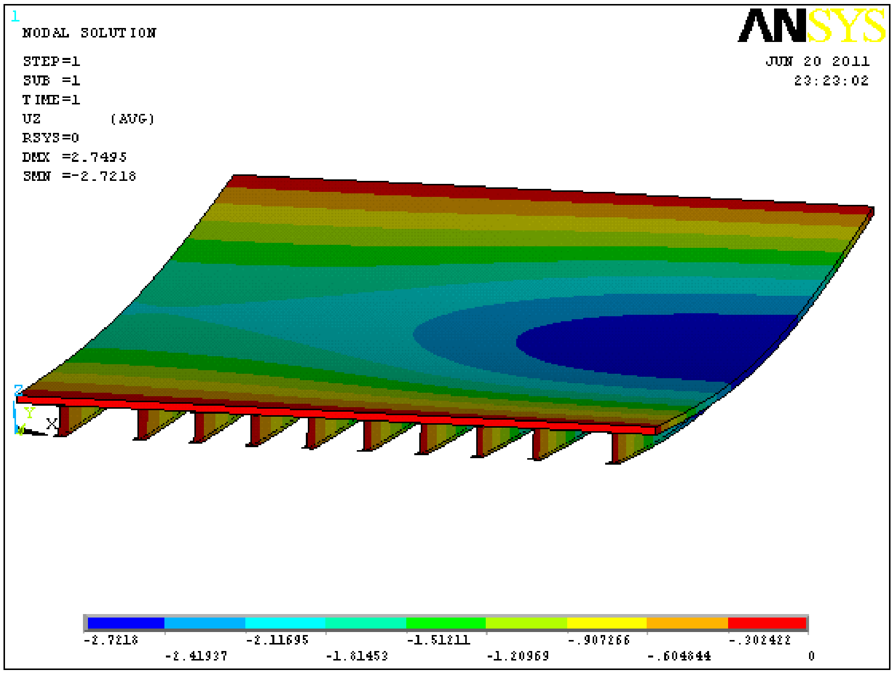

Figure 32
Steel span deformation under service limit state before rehabilitation

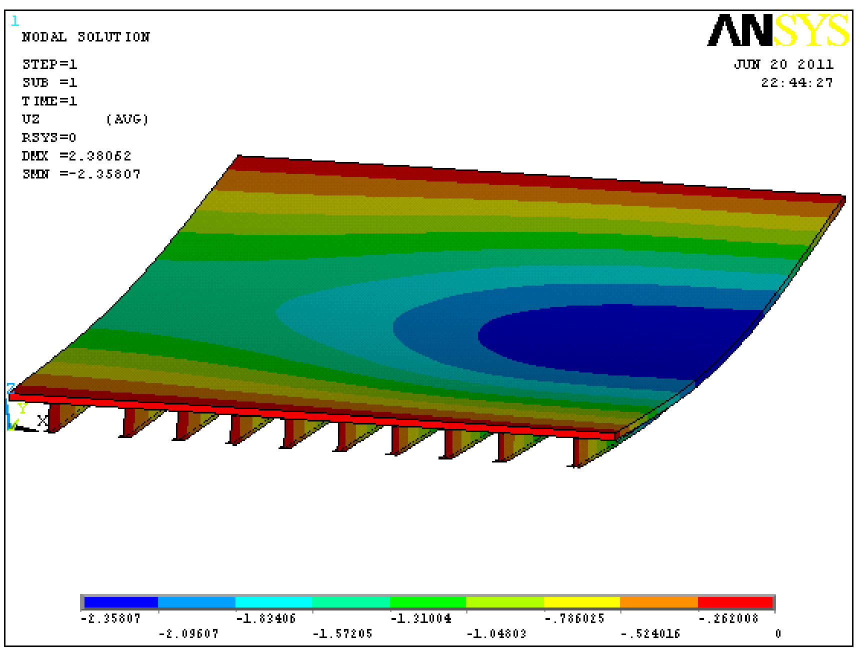

Figure 33
Steel span deformation under service limit state after rehabilitation

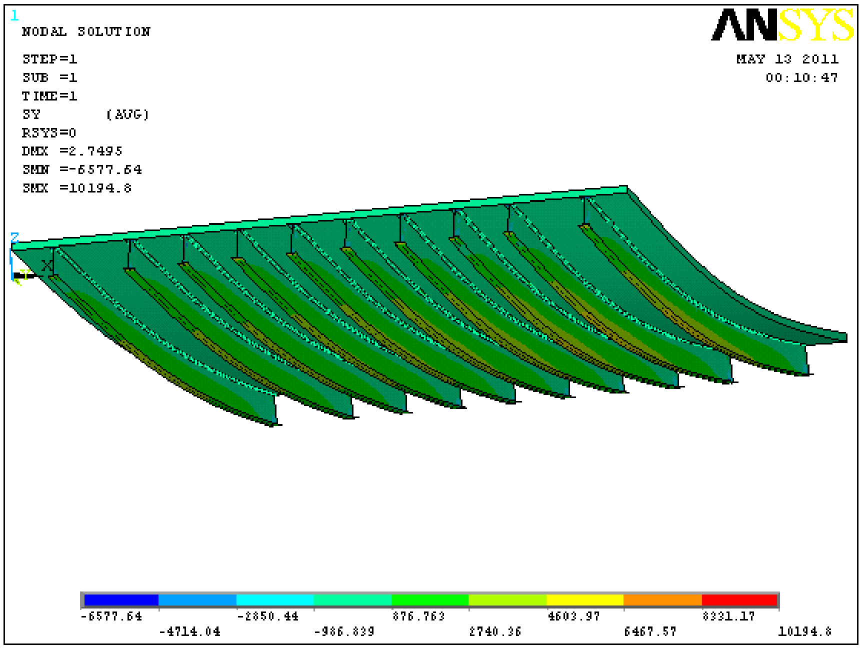

Figure 34
Steel girders longitudinal stress under service limit state before rehabilitation

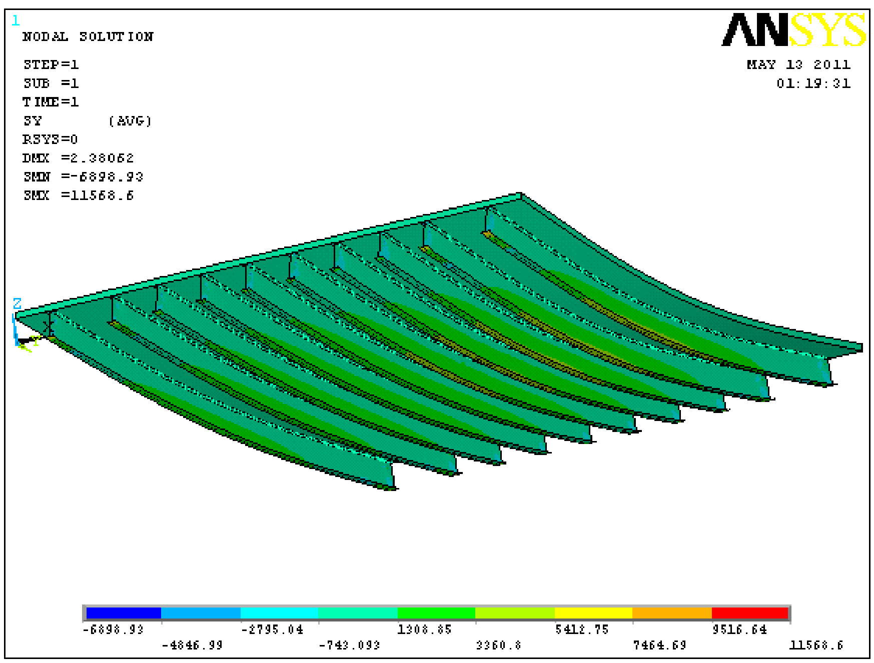

Figure 35
Steel girders longitudinal stress under service limit state after rehabilitation

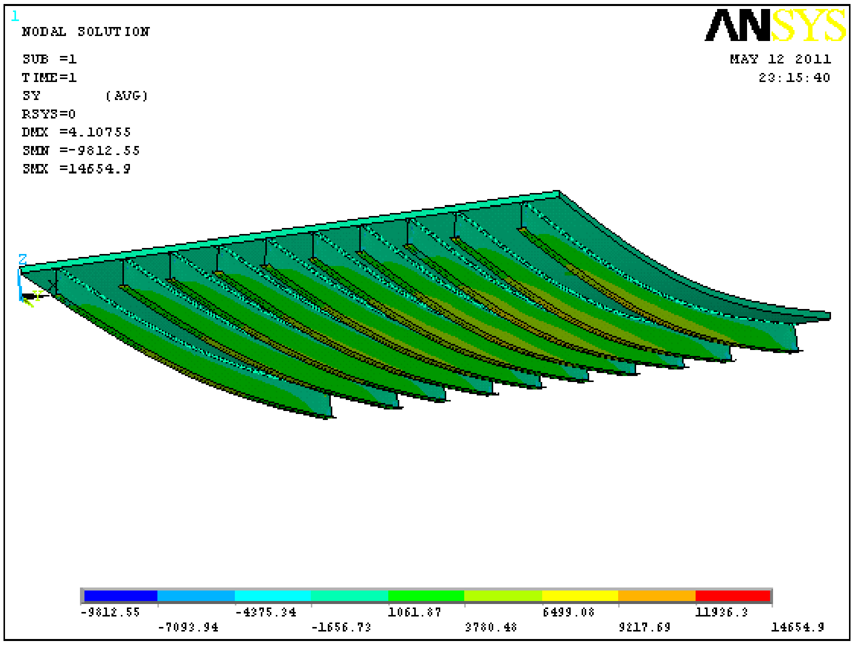

Figure 36
Steel girders longitudinal stress under strength limit state before rehabilitation

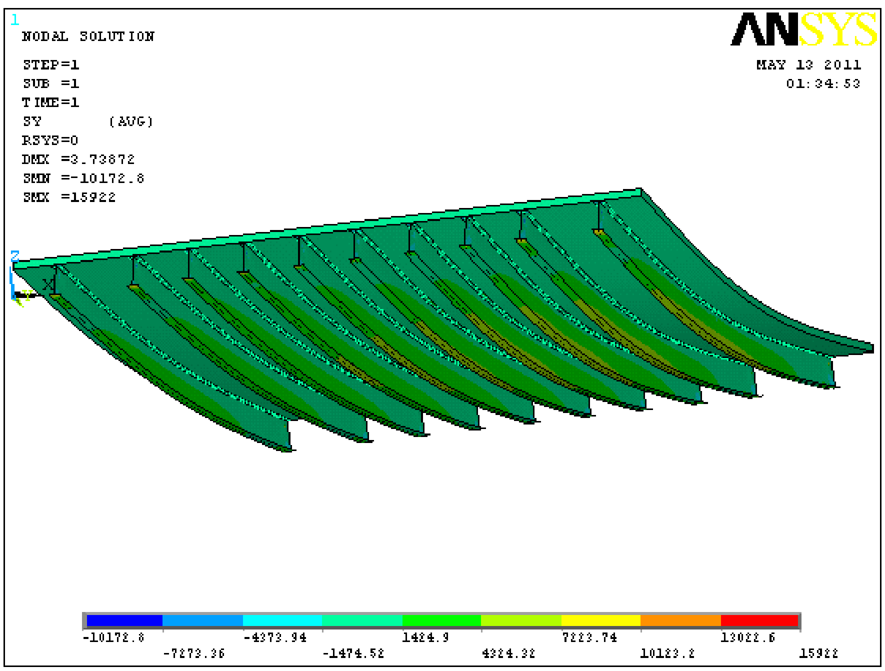

Figure 37
Steel girders longitudinal stress under strength limit state after rehabilitation

CONCLUSIONS

A comprehensive review of the current work on bridge strengthened with prestressed FRP composite was presented in this report. Different types of rehabilitation methods with various commercial products were introduced. The performance of the rehabilitation of existing bridges with prestressed external FRP materials was evaluated by tentative design and 3-D finite element analysis. A case study demonstrated the design procedure for rehabilitation with bonded post-pretention prestressed CFRP laminates. In the case study, the performance of the selected bridge was evaluated before and after the rehabilitation. The following conclusions can be made:

1. The safety factor of every span of an existing bridge can be non-uniform. In this case, the flexural capability of the 64-ft., 6-in. (19.66-m) span steel I-beam is sufficient to meet the current traffic requirement, but not the 38-ft. (11.58-m) cast-in-place concrete T-beam approach span.
2. The stress of the steel I-beam span girders under the service load is beyond 55 percent of steel yield strengthf_y.
3. Rehabilitation with externally prestressed CFRP laminates is a feasible way to enhance the flexural capability. For the cast-in-place concrete tee beam approach span, the ultimate capability is improved by 39 percent; for the span steel I-beam, the stress under the service load can be reduced from 75 percent to less than 55 percent of the steel yield strengthf_y.
4. The longitudinal bottom fiber stresses calculated in the 3-D finite element analysis is smaller than that derived from a tentative design following code specifications.

RECOMMENDATIONS

From the previous analysis and results, the following recommendations can be made. Since the loss of the prestress in the CFRP materials is determined by the type of the products and method of construction, a special field test is needed to determine the stress variation during construction. Although durability has been cited as a strong selling point for FRP composite materials, polymer matrices degrade when subjected to environmental attacks or long-term loading. These attacks include, but are not limited to, moisture, alkali, thermal, freeze/thaw, creep/stress relaxation, fatigue, ultraviolet radiation (UV), fire, and, of course, the various combinations of the environment and loadings. However, not all the attacks or their combinations can be found for a specific application and not all of them or their combinations have the same detrimental effect. It is expected that a long-term field monitoring of the girders to determine the actual durability under field conditions over extended periods of time is essential for the optimal design of FRP composites for use in civil infrastructures.

ACRONYMS, ABBREVIATIONS, & SYMBOLS

AASHTO	American Association of State Highway and Transportation Officials
ASCE	American Society of Civil Engineers
CFCC	Carbon Fiber Composite Cables
FEM	Finite Element Model
ft.	foot (feet)
FOS	Fiber Optic Sensor
FRP	Fiber Reinforced Polymer
GFRP	Glass Fiber Reinforced Polymer
in.	inch (es)
kip	kilo Pounds
LADOTD	Louisiana Department of Transportation and Development
lb.	pound (s)
LTRC	Louisiana Transportation Research Center
m	meter (s)
mm	millimeter
NSM	near surface mounted
RC	Reinforced Concrete

REFERENCES

1. TRIP, The Road Information Program. "Showing Their Age: The Nation's Bridges at 40 Strategies to Improve the Condition of Our Bridges and Keep Them in Good Shape," Washington, DC., 2002.

2. The Status of the Nation's Highway, Bridges and Transit: Condition and Performance, Report of the Secretary of Transportation to U.S. Congress, 1993.

3. ACI Committee 440, ACI 440.2R-02 Guide for the design and Construction of Externally Bonded FRP Systems for Strengthening Concrete Structures, USA, 2002.

4. ACI Committee 440, ACI 440.2R-04 Prestressing Concrete Structures with FRP Tendons, USA, 2004.

5. Task Group 9.3, Externally Bonded FRP Reinforcement for RC Structures, fib CEB-FIB Bulletin 14, Switzerland, 2001.

6. Woo, S.K., Nam, J.W., Kim**,** J.H, Han, S.H., and Byun, K.J. "Suggestion of Flexural Capacity Evaluation and Prediction of Prestressed CFRP Strengthened Design," *Engineering Structures*, 2008. 30(12): pp. 3751-3763.

7. Mukherjee, A. and Rai, G.L. "Performance of Reinforced Concrete Beams Externally Prestressed with Fiber Composites," *Construction and Building Materials*, 2009. 23(2): pp. 822-828.

8. Ceroni, F., "Experimental Performances of RC Beams Strengthened with FRP Materials" *Construction and Building Materials*, 2010. 24(9): pp. 1547-1559.

9. Badawi, M. and Soudki, K. "Flexural Strengthening of RC Beams with Prestressed NSM CFRP Rods - Experimental and Analytical Investigation," *Construction and Building Materials*, 2009. 23(10): pp. 3292-3300.

10. Czaderski, C. and Motavalli, M. "40-Year-Old Full-scale Concrete Bridge Girder Strengthened with Prestressed CFRP Plates Anchored Using Gradient Method," *Composites Part B: Engineering*, 2007. 38(7-8): pp. 878-886.

11. Rosenboom, O., Hassan, T.K., and Rizkalla, S. “Flexural Behavior of Aged Prestressed Concrete Girders Strengthened with Various FRP Systems*,” Construction and Building Materials*, 2007. 21(4): pp. 764-776.

12. Saqan, E. and Rasheed, H., “Simplified Nonlinear Analysis to Compute Neutral Axis Depth in Prestressed Concrete Rectangular Beams,” *Journal of the Franklin Institute*, in press.

13. Xue, W., Tan, Y., and Zeng, L. “Flexural Response Predictions of Reinforced Concrete Beams Strengthened with Prestressed CFRP plates*,” Composite Structures*, 2010. 92(3): pp. 612-622.

14. Stoll, F., Saliba, J.E. and Casper, L.E. “Experimental Study of CFRP-Prestressed High-strength Concrete Bridge Beams,” *Composite Structures*, 2000. 49(2): pp. 191-200.

15. Maalej, M. and Leong, K.S., “Engineered Cementitious Composites for Effective FRP-strengthening of RC beams*,” Composites Science and Technology*, 2005. 65(7-8): pp. 1120-1128.

16. Yang, D.-S., Park, S.K. and Neale, K.W. “Flexural Behaviour of Reinforced Concrete Beams Strengthened with Prestressed Carbon Composites*,” Composite Structures,* 2009. 88(4): pp. 497-508.

17. Pham, H. and Al-Mahaidi, R. “Assessment of Available Prediction Models for the Strength of FRP Retrofitted RC Beams,” *Composite Structures*, 2004. 66(1-4): pp. 601-610.

18. Garden, H.N. and Hollaway, L.C. “An Experimental Study of the Failure Modes of Reinforced Concrete Beams Strengthened with Prestressed Carbon Composite Plates*,” Composites Part B: Engineering*, 1998. 29(4): pp. 411-424.

19. Wu, Z.J. and Davies, J.M. “Mechanical Analysis of a Cracked Beam Reinforced with an External FRP Plate,” *Composite Structures*, 2003. 62(2): pp. 139-143.

20. Almusallam, T.H. and Al-Salloum, Y.A. “Ultimate Strength Prediction for RC Beams Externally Strengthened by Composite Materials” *Composites Part B: Engineering*, 2001. 32(7): pp. 609-619.

21. Gunes, O., Buyukozturk, O., and Karaca, E. "A Fracture-based Model for FRP Debonding in Strengthened Beams*," Engineering Fracture Mechanics*, 2009. 76(12): pp. 1897-1909

22. Smith, S.T. and Teng, J.G. "FRP-strengthened RC Beams. I: Review of Debonding Strength Models*," Engineering Structures*, 2002. 24(4): pp. 385-395.

23. Smith, S.T. and Teng, J.G. "FRP-strengthened RC Beams. II: Assessment of Debonding Strength Models*" Engineering Structures*, 2002. 24(4): pp. 397-417.

24. Chen, J.F. and Pan, W.K. "Three Dimensional Stress Distribution in FRP-to-Concrete Bond Test Specimens," *Construction and Building Materials*, 2006. 20(1-2): pp. 46-58.

25. Arockiasamy, M., Chidambaram, S., Amer, A., and Shahawy, M. "Time-Dependent Deformations of Concrete Beams Reinforced with CFRP Bars," *Composites Part B: Engineering*, 2000. 31(6-7): pp. 577-592.

26. Youakim, S.A. and Karbhari,V.M. "An Approach to Determine Long-term Behavior of Concrete Members Prestressed with FRP Tendons*," Construction and Building Materials*, 2007. 21(5): pp. 1052-1060.

27. Zou, P.X.W. and Shang, S. "Time-Dependent Behaviour of Concrete Beams Pretensioned by Carbon Fibre-Reinforced Polymers (CFRP) tendons*," Construction and Building Materials*, 2007. 21(4): pp. 777-788.

28. Chen, S. and Gu, P. "Load Carrying Capacity of Composite Beams Prestressed with External Tendons under Positive Moment," *Journal of Constructional Steel Research*, 2005. 61(4): pp. 515-530.

29. Park, S., Kim, T., Kim, K., and Hong, S.N. "Flexural Behavior of Steel I-beam Prestressed with Externally Unbonded Tendons," Journal of Constructional Steel Research, 2010. 66(1): pp. 125-132.

30. Park, R. and Paulay, T. *Reinforced concrete structures*. 1975, New York: Wiley. xvii, 769 p.

31. Alkhairi, F.M. and Naaman, A.E. "Analysis of Beams Prestressed with Unbonded Internal or External Tendons," *Journal of Structural Engineering*, 1993. 119(9): pp. 2680-2700.

32. Aravinthan, T. “Prediction of the Ultimate Flexural Strength of Externally Prestressed PC Beams,” *Transactions of the Japan Concrete Institute*, 1997. 19: pp. 225-230.

33. American Association of State Highway and Tranporttion Officials (AASHTO). Manual for Condition Evaluation of Bridges, American Association of State Highway and Tranporttion Officials, Washington, D.C., 2001.

APPENDIX

As mentioned in the present report, FRP materials are usually fabricated as various products such as strands, rods, laminates, strips, and fabrics. The type of products determined the methods of construction in the civil engineering field. FRP laminates, strips, and fabrics are usually glued at the surface of the concrete or steel components to enhance their service performance. All of them are used as rehabilitation materials for existing structures. They can be prestressed or non-prestressed when they are glued to the component surfaces.

FRP rods, bars, and strands, on the other hand, can be used for constructing new structures or strengthening existing structures. They can be used as internal reinforcements when constructing a component, and they can totally replace steel reinforcements, prestressed or non-prestressed. To strengthen existing structures, FRP rods or bars can be connected to structure components through anchorage. The external usage of FRP rods are usually realized with post-tensioned prestressed techniques. The rehabilitation design using prestressed rods is presented next.

Commercial CFRP Rods

Several properties such as high strength, excellent corrosion, and fatigue resistance, make CFRP material one of the best choices of external post-tensioning tendons. Leadline™ and Carbon Fiber Composite Cables (CFCC) are two kinds of commercially available tendons. The properties of these two CFRP tendons are listed in Table 14. According to previous engineering experience, Leadline™ tendons are typically used as pre-tensioning strands, and CFCCs are typically used as post-tensioning strands.

Table 14
Properties of CFRP rods

Property	Leadline™	CFCC
Fiber	Carbon	Carbon
Resin	Epoxy	Epoxy
Fiber volume ratio	0.65	0.65
Density, g/cm³	1.53	1.65
Longitudinal tensile strength, Gpa	2.25 to 2.55	1.8 to 2.1
Longitudinal modulus, Gpa	142 to 150	137
Bond Strength, Mpa	4 to 20	7 to 11
Maximum transverse strain, %	1.3 to 1.5	1.57
Relaxation ration at room temperature, % loss from jacking stress	2 to 3	0.5 to 1 at 102 h

CFCC strands, products of Tokyo Rope, are world-wide used tendons in the civil engineering field. Tendons and anchorages are usually provided together by manufactures. The shape and size of the terminal fixer are shown in Figure 38 and Table 15.

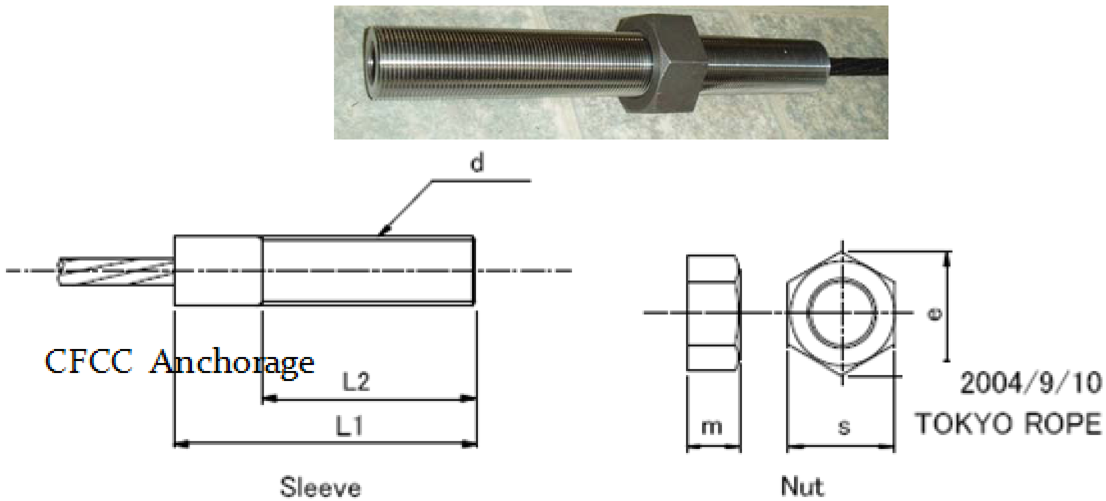

Figure 38
Terminal fixer

Table 15
Size of terminal fixer

CFCC				Sleeve					Nut					
Configuration diameter (mm)	Area in²	Capacity kips	Density lb/f	thread d	L1		L2		M		s		e	
					mm	In	mm	in	mm	in	mm	in	mm	in
CFCC 1X7 7.5 φ	0.047	12.81	0.043	M 22X2.5	170	6.69	140	5.51	18	0.71	32	1.26	37	1.46
CFCC 1X7 10.5 φ	0.086	23.38	0.077	M 33X3.5	200	7.87	160	6.3	26	1.02	50	1.97	57.7	2.27
CFCC 1X7 12.5 φ	0.118	31.92	0.101	M 36X4	250	9.84	210	8.27	29	1.14	55	2.17	63.5	2.5
CFCC 1X7 15.2 φ	0.176	44.74	0.152	M 39X4	280	11	240	9.45	31	1.22	60	2.36	69.3	2.73
CFCC 1X7 17.2 φ	0.232	58.8999	0.195	M 45X4.5	300	11.8	250	9.84	36	1.42	70	2.76	80.8	3.18
CFCC 1X19 20.5 φ	0.32	71.0396	0.276	M 52X5	300	11.8	240	9.45	42	1.65	80	3.15	92.4	3.64
CFCC 1X19 25.5 φ	0.472	104.986	0.407	M 60X5.5	350	13.8	290	11.4	48	1.89	90	3.54	104	4.09
CFCC 1X19 28.5 φ	0.622	133.537	0.522	M 68X6	400	15.7	330	13	54	2.13	100	3.94	115	4.53
CFCC 1X37 35.5 φ	0.916	189.064	0.796	M 85X6	430	16.9	340	13.4	68	2.68	120	4.72	139	5.47
CFCC 1X37 40 φ	1.208	240.546	1.013	M 95X6	500	19.7	400	15.7	76	2.99	135	5.31	156	6.14

ACI 440.4R-04 proposed a method to calculate ultimate nominal flexural capability of prestressing concrete structures with FRP tendons. For unbounded prestressed members, the stress in the prestressing tendons at failure of the beam must be determined using the following relationships:

$$f_p = f_{pe} + \Delta f_p \tag{62}$$

where, f_{pe} is the effective prestress in the tendon when the beam carries only the dead load after the prestress losses have occurred, and Δf_p is the stress increase above f_{pe} due to any additional applied load. The Δf_p can be derived by using strain compatibility and, by assuming linear elastic behavior of the tendon, the change in stress Δf_p in the unbounded tendon is given by:

$$\Delta f_p = \Omega_u E_p \varepsilon_{cu} \left(\frac{d_p}{c_u} - 1\right) \tag{63}$$

where, ε_{cu} is the strain in the extreme compression fiber at ultimate, and c_u is the depth of the neutral axis at ultimate. According to Alkhaini's research, the strain reduction coefficient at ultimate, Ω_u can be determined by *[31]*

$$\Omega_u = \frac{3.0}{(L/d_p)} \quad \text{(for two-point or uniform loading)} \tag{64}$$

Concrete Girder Span

The existing flexural capacities of exterior and interior-exterior girders have been calculated in the report. It shows that the flexural capacities do not meet the present traffic requirements. In this case, to enhance the flexural capacities, two CFCC 25.5 φ tendons were added for each girder. They are located at a position of 3 in. (0.08 m) under the bottom of the girder and are shown in Figure 39. The nominal moment of the rehabilitated girders can be derived through the equilibrium equation. The allowable tendon stress at jacking for carbon tendons is $0.7f_{pu}$.

The calculation of the exterior girder is shown below:

Given information for rehabilitation: section area of CFRP rods $A_p = 2 \times 0.472 in^2$, ultimate strength if CFRP rods $f_{pu} = 2.223 \times 10^5 psi$, $E_f = 1.8 \times 10^7 psi$ initial pulling stress $f_i = 0.35 f_{pu}$.

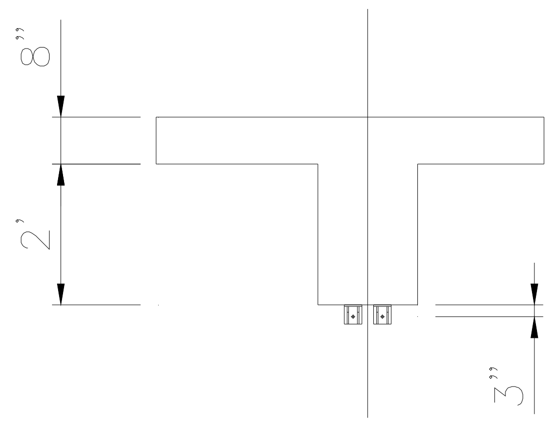

Figure 39
Set up of CFRP rods in concrete span

Exterior Girder

Prestress loss calculation

Modular ratio: $n = E_{frp}/E_c = 5.766$

Elastic shortening: $\Delta f_{es} = nf_{cp}(P_i/A + P_i e/S_p - M_d/S_p) = 532\,psi$

Creep: assume 2 times initial elastic shortening $\Delta f_r = C_c \Delta f_{es} = 1{,}065\,psi$

Shrinkage: assume 0.0006 net strain at time of testing $\Delta f_s = \mathcal{E}_s E_p = 10{,}800\,psi$

Relaxation: $\Delta f_r = 0.03 f_{pi} = 4{,}668 psi$

Total losses: $\Delta f_{es} + \Delta f_r + \Delta f_s + \Delta f_r = 17{,}065 psi = 0.219 f_i$

Effective prestress: $f_{pe} = 0.35 f_{pu} - losses = 60{,}737 psi$

Final prestress $= m A_p f_{pe} = 57{,}371 lbf$

Check service level stress at mid-span:

Initial stresses

Top= $P_i/A - P_e e/S_t + M_d/S_t = 166.231\,psi$

Bottom= $P_e/A - P_e e/S_b + M_d/S_b = -137.490\,psi$

Final stresses

Top= $P_i/A - P_e e/S_t + M_d/S_t - M_l/S_b = 205.131\,psi$

Bottom = $P_e/A - P_e e/S_b - M_d/S_b - M_l/S_b = -2{,}293\,psi$

Check strength capacity

Strain reduction coefficient at ultimate $\Omega_u = \frac{3}{L/d_p} = 0.23$

Depth of concrete compressing zone at ultimate state is c_u. Assume neutral axis is in the flange, by solving the equilibrium equation.

$0.85 f_c b_{eff} - A_s f_y - A_p \times \left(f_e + \Omega_u \times E_p \times \mathcal{E}_{cu} \times \left(d_p/c_u - 1\right)\right) = 0$

$c_u = 3.087\ in < 8\ in$

the neutral axis in the flange is confirmed.

$a_e = 0.85 c_u = 2.624\ in$

CFRP stress at ultimate $f_p = f_e + \Omega_u \times E_p \times \mathcal{E}_{cu} \times \left(d_p/c_u - 1\right) = 1.893 \times 10^5\ psi$

nominal flexural capacity

$M_{n\_e} = f_p \times A_p \times \left(35\ in - \frac{a_e}{2}\right) + A_s f_y \times \left(d_e - \frac{a_e}{2}\right) = 1325\ kip\ ft$

$0.9 M_{n\_e} > M_{u\_e}$

Interior-exterior Girder

Prestress loss calculation:

Modular ratio: $n = E_{frp}/E_c = 5.766$

Elastic shortening: $\Delta f_{es} = n f_{cp}(P_i/A + P_i e/S_p - M_d/S_p) = 541\ psi$

Creep: assume 2 times initial elastic shortening $\Delta f_r = C_c \Delta f_{es} = 1{,}081\ psi$

Shrinkage: assume 0.0006 net strain at time of testing $\Delta f_s = \mathcal{E}_s E_p = 10{,}800\ psi$

Relaxation: $\Delta f_r = 0.03 f_{pi} = 4{,}668 psi$

Total losses: $\Delta f_{es} + \Delta f_r + \Delta f_s + \Delta f_r = 17{,}090 psi = 0.220\ f_i$

Effective prestress: $f_{pe} = 0.35 f_{pu} - losses = 60{,}712\ psi$

Final prestress $= m A_p f_{pe} = 57{,}347\ lbf$

Check service level stress at mid-span:

Initial stresses

Top= $P_i/A - P_e e/S_t + M_d/S_t = 176\ psi$

Bottom= $P_e/A - P_e e/S_b + M_d/S_b = -108\ psi$

Final stresses

Top= $P_i/A - P_e e/S_t + M_d/S_t - M_l/S_b = 763\ psi$

Bottom $= P_e/A - P_e e/S_b - M_d/S_b - M_l/S_b = -776\ psi$

Check strength capacity

Strain reduction coefficient at ultimate $\Omega_u = \frac{3}{L/d_p} = 0.23$

Depth of concrete compressing zone at ultimate state is c_u

assume neutral axis is in the flange, by solving the equilibrium equation

$0.85 f_c b_{eff} - A_s f_y - A_p \times \left(f_e + \Omega_u \times E_p \times \mathcal{E}_{cu} \times \left(d_p/c_u - 1\right)\right) = 0$

$c_u = 2.891\ in < 8\ in$.   The neutral axis in the concrete deck is confirmed.

$a_e = 0.85c_u = 2.624\ in$

CFRP stress at ultimate $f_p = f_e + \Omega_u \times E_p \times \mathcal{E}_{cu} \times \left(d_p/c_u - 1\right) = 1.763 \times 10^5\ psi.$

Nominal flexural capacity

$$M_{n\_i} = f_p \times A_p \times \left(35\ in - \frac{a_e}{2}\right) + A_s f_y \times \left(d_e - \frac{a_e}{2}\right) = 1174\ kip\ ft$$

$0.9M_{n\_i} > M_{u\_i}$

The nominal moments for exterior and interior-exterior girders rehabilitated with externally prestressed CFRP tendons meet the requirements of current traffic.

Steel Girder Span

According to the calculations in the report, the steel girder ultimate flexural capacities satisfy the traffic requirements, but under the service state, the maximum stress at the bottom fiber exceeds the limitation of 0.55 f_y where f_y is the yield strength of steel. The aim of the rehabilitation is to ensure the stress under the service state is less than $0.55f_y$.

In order to reduce the steel girder stress under the service load, the steel I-beam girder can be rehabilitated with externally prestressed CFRP rods too. Like the concrete span, two CFCC25.5 φ tendons were added to the exterior and interior-exterior girders. They are located at a position 3 in. (0.08 m) above the bottom of the girder as shown in Figure 40. The nominal moment of the rehabilitated girders can be derived through equilibrium equation. The allowable tendon stress at jacking for carbon tendons is $0.7f_{p\_u}$.

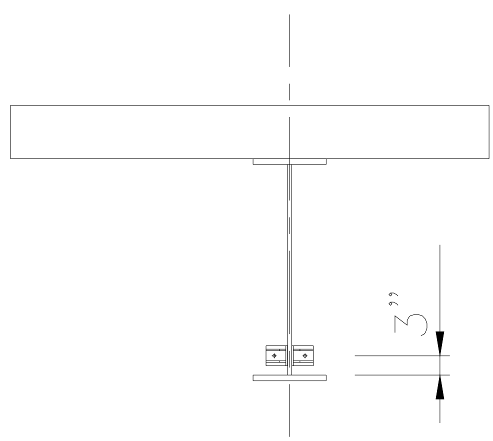

Figure 40
Set up of CFRP rods in steel span

The calculation of the exterior girder is shown below:

Given information for rehabilitation: the section area of CFRP rods $A_p = 2 \text{ x } 0.472\ in^2$, ultimate strength if CFRP rods $f_{pu} = 2.223 \text{ x } 10^5\ psi$, $E_f = 1.8 \text{ x } 10^7\ psi$. Since there is limited information of prestress loss of CFRP rods applied on steels, it is assumed that the effective prestress in the rods when the beam carries only the dead load after the prestress losses have occurred is assumed to be 0.5 f_u; f_u is the ultimate stress of CFRP tendons.

Stress Under Service Load Combination

The maximum steel girder tension stress under service can be obtained from following equation

$$f_s = \frac{M_{beam}}{S_b} + \frac{M_{deck}}{S_{b3n}} + \frac{M_{bar}}{S_{b3n}} + \frac{M_{FW}}{S_{b3n}} + \frac{M_{truck} I_m DF}{S_{bn}} + \frac{M_{lane} I_m}{S_{bn}} - \frac{T_{ten}}{A_{c3n}} - \frac{T_{ten}(y_{b3n} - 2in)}{S_{b3n}}$$

where, S_b, S_{b3n} and S_{bn} are section modulus of steel beam, modulus of composite section for long-term and short-term, respectively.

For exterior girders, $f_{s\_e} = 23.392\ ksi = 0.57 f_y$

and for interior-exterior girders $f_{s\_i} = 22.149\ ksi = 0.54 f_y$

Nominal Flexural Capacity of Composite Girders

A plastic analysis is conducted. For exterior girders, assume the plastic axis is at the bottom of the concrete deck, then:

compression force in concrete: $F_c = 0.85 \times f_c \times b_f \times d_c = 1.714 \times 10^7\ lbf$

tension force in steel beam: $F_{T\_t} = f_y \times A_{st} + f_e \times A_p = 1.729 \times 10^7\ lbf$

Since the compressive force in concrete is less than the tension force in the steel beam, the plastic axis is located in the steel beam. Using the equilibrium equation, the plastic axis was found to be located in the top flange of the steam beam, 0.06 in. (0.002 m) from top surface of the steel beam top flange. It is so close to the bottom surface of the concrete deck, for simplification, it is reasonable to assume that the plastic axis is located there.

The nominal flexural capacity is derived from the diagram shown in Figure 41.

$$M_{n\_e} = F_c \times 4\ in + f_y \times A_{st} \times \frac{d}{2} + f_e \times A_p \times (d - 3in) = 3.742 \times 10^7\ in\ lbf$$

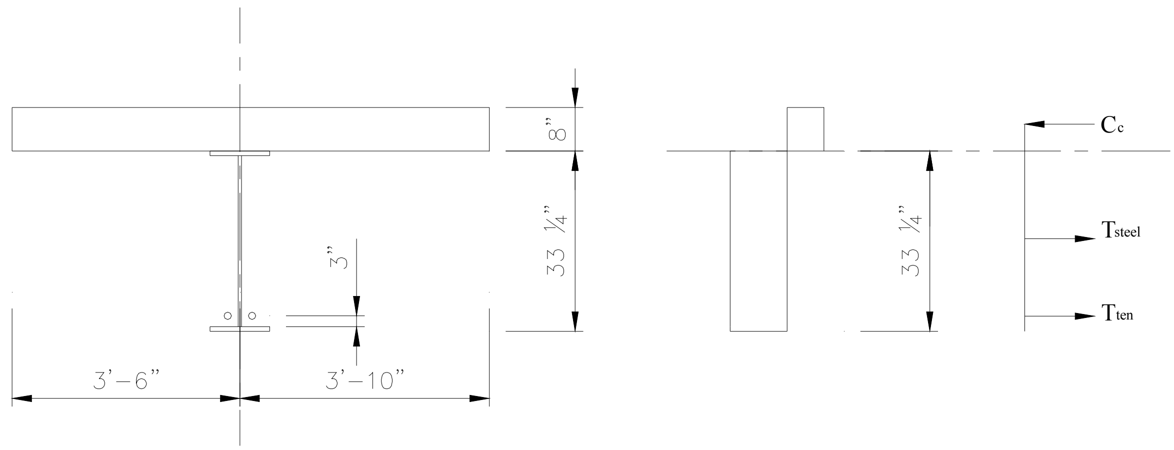

Figure 41
Plastic analysis diagram of exterior girder

For interior-exterior girders, assume the plastic axis is at the bottom of the concrete deck, then we have:

compression force in concrete: $F_c = 0.85 \times f_c \times b_f \times d_c = 1.224 \times 10^6 \; lbf$

tension force in steel beam: $F_{T\_t} = f_y \times A_{st} + f_e \times A_p = 1.729 \times 10^6 \; lbf$

Since the compressive force in concrete is less than the tension force in the steel beam, the plastic axis is located in the steel beam. Using the equilibrium equation, the plastic axis was found to be located in the web of the steel beam, 1.038 in. (0.026 m) from top surface of the steel beam top flange.

The nominal flexural capacity is derived from the diagram shown in Figure 42.

$M_{n\_i} = 3.55410^7 \; in \; lbf$

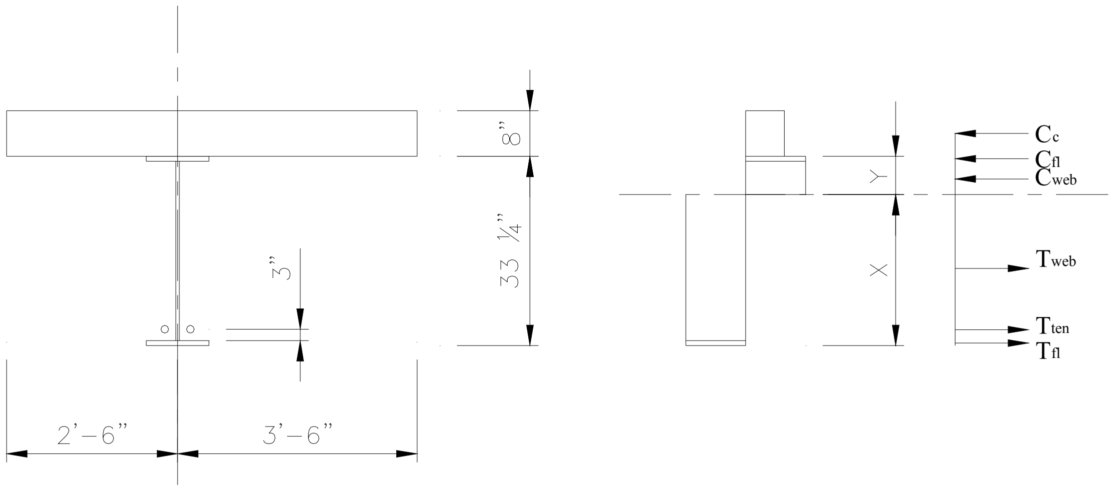

Figure 42
Plastic analysis diagram of interior-exterior girder

Cost Estimates of CFRP Rods

The information to estimate the cost of CFRP strands is limited. There is little information on the exact price of CFCC 1×19 28.5Φ, which was selected for the project. An estimate of the price of CFRP rods is listed below:

US \$18.00 per meter for CFCC 1×7 12.5Φ
US \$25.00 per meter for CFCC 1×7 15.2Φ

To estimate the cost of CFRP, it is estimated that the price is US \$60.00 per meter for CFCC1×19 25.5Φ. The above prices are based on current exchange rate of Yen 100 per US \$1.00 and actual transaction price will change subject to exchange rate at the time of purchase contract. In addition, the cost for ocean transportation, import duty, and inland transportation in USA shall be added to the above Japan price. In this cost estimation, US \$65.00 per meter is adopted to include some unexpected expenses. The cost estimate of CFRP strands (material only) for the entire bridge is listed in Table 16. As a demonstration, four beams (two exterior beams and two in-exterior beams) of the 64 ft. and 6 in. (19.66 m) steel I-beam span and a typical 38 ft. (11.58 m) approach span can be rehabilitated. The material cost of the demonstration project is listed in Table 17.

Table 16
CFRP strands cost estimate of entire bridge

Girder location		Number of spans	Span Length (ft)	Number of girders	Strand length (ft)	Cost (USD)
approach spans	exterior	20	38	2	30x2	47548.8
	in-exterior	20	38	2	30x2	47548.8
	interior	20	38	6	30x2	142646.4
main crossing (I)	exterior	1	64.5	2	56x2	4437.89
	in-exterior	1	64.5	2	56x2	4437.89
	interior	1	64.5	6	56x2	13313.7
main crossing (II)	exterior	2	47	2	39x2	6181.34
	in-exterior	2	47	2	39x2	6181.34
	interior	2	47	6	39x2	18544
main crossing (III)	exterior	2	38	2	30x2	4754.88
	in-exterior	2	38	2	30x2	4754.88
	interior	2	38	6	30x2	14264.6
					Sum=	314615

Table 17
CFRP strands cost estimate of demonstration engineering

Girder location		Span Length (ft)	Number of girders	Strand length (ft)	Cost (USD)
approach spans	exterior	38	2	30x2	2237.44
	in-exterior	38	2	30x2	2237.44
64' I-Steel beam	exterior	64	2	56x2	4437.89
	in-exterior	64	2	56x2	4437.89
				Sum=	13630.66

This public document is published at a total cost of $250
42 copies of this public document were published in this first printing at a cost of $250. The total cost of all printings of this document including reprints is $250. This document was published by Louisiana Transportation Research Center to report and publish research findings as required in R.S. 48:105. This material was duplicated in accordance with standards for printing by state agencies established pursuant to R.S. 43:31. Printing of this material was purchased in accordance with the provisions of Title 43 of the Louisiana Revised Statutes.